2020

Biodegradable Biomaterials as Suitable Alternatives to Water Treatment Technologies

Most Farzana Yesmin
South Dakota State University

BIODEGRADABLE BIOMATERIALS AS SUITABLE ALTERNATIVES TO WATER TREATMENT TECHNOLOGIES

By

MOST FARZANA YESMIN

A thesis submitted in partial fulfillment of the requirements for the

Master of Science

Department of Dairy and Food Science

Specialization in Food Science

South Dakota State University

2020

THESIS ACCEPTANCE PAGE

Most Farzana Yesmin

This thesis is approved as a creditable and independent investigation by a candidate for the master's degree and is acceptable for meeting the thesis requirements for this degree. Acceptance of this does not imply that the conclusions reached by the candidate are necessarily the conclusions of the major department.

Srinivas Janaswamy
Advisor Date

Vikram Mistry
Department Head Date

Dean, Graduate School Date

THIS THESIS IS DEDICATED TO MY PARENTS

ACKNOWLEDGMENTS

I would like to express my heartfelt gratitude to Dr. Srinivas Janaswamy for his continuous support, motivation, guidance, and supervision during this thesis work. I also want to express my sincere gratitude and appreciation to advisory committee members Dr. Vikram Mistry and Dr. Cody Christensen for their continuous encouragement and direction along the way. I would like to thank Dr. Laurent Ahiablame for his support and scientific input in this thesis work. Thanks to John Maursetter to assist me in analyzing water samples. I am also thankful to Dr. Omathanu Perumal and Dr. Kasiviswanathan Muthukumarappan for providing me access to ATR-FTIR and DSC instruments respectively to characterize my samples. I also would like to thank all previous and current lab members of Dr. Janaswamy research group for their help.

I owe my gratitude and utmost respect to my wonderful parents for their unconditional and sincere love, support, and encouragement. I am forever indebted to my dear husband, for his love, patience, and exceptional forgiveness that provided me the strength and confidence to complete my thesis.

I would like to thank the "South Dakota Nutrient Research and Education Council (NREC)" for supporting this research project.

Lastly, but not least of all, I will always remain grateful to the Department of Dairy and Food Science at South Dakota State University, for supporting my MS study.

TABLE OF CONTENTS

LIST OF FIGURES

LIST OF TABLES

SYMBOLS AND ABBREVIATIONS

%	Percent
°	Degree
˚C	Degree Centigrade
>	Greater- than
<	Less-than
mg	Milligram
g	Gram
ANOVA	Analysis of Variance
Al	Aluminum
$CaCl_2$	Calcium Chloride
Cu	Copper
Al^{3+}	Aluminum (III)
Fe	Iron
$CuCl_2$	Copper chloride
Fe^{3+}	Iron (III)
Ca	Calcium
Fe^{2+}	Iron (II)
Ni	Nickel
Zn	Zinc
Sr	Strontium

α	Alpha
FTIR	Fourier-transform infrared spectroscopy
DSC	Differential Scanning Calorimetry
mL	Milliliter
p-value	Probability value
SE	Standard Error
J/g	Joule/gram
cm^{-1}	Per centimeter
-C-O-O-	Carboxyl group
-C-O-	Carbon-oxygen
-C-OH	Carbon-Hydroxyl group
-OH	Hydroxyl group

ABSTRACT

BIODEGRADABLE BIOMATERIALS AS SUITABLE ALTERNATIVES TO WATER TREATMENT TECHNOLOGIES

MOST FARZANA YESMIN

2020

Nitrates and phosphates are essential nutrients for plants growth. Their excess presence in water, however, could cause eutrophication affecting the water quality and altering the aquatic ecosystem. Algal blooms and the presence of toxins such as microcystin in freshwater bodies are hazardous to humans, animals, and wildlife. Conventional technologies such as ion exchange, distillation, reverse osmosis, and bioreactors aid immensely to remove nutrients; however, they are expensive. Furthermore, building new nitrate and phosphate treatment units, maintenance and post-disposal are costly too. In this regard, there exists an unmet need for alternative processes that are renewable and cost-effective to treat contaminated water.

Herein, a novel opportunity based on inexpensive and widespread polysaccharides, *e.g.* alginate, has been developed to capture nitrate and phosphate from water and improving water quality. Alginate beads have been prepared in the presence of divalent (Ca^{2+}, Fe^{2+}, Ni^{2+}, Cu^{2+}, $Zn^{2+,}$ and Sr^{2+}) and trivalent (Al^{3+} and Fe^{3+}) cations. The maximum absorption capacity of nitrate and phosphate by the alginate beads has been established using 5, 10, 25 mg/L of nitrate and 1, 5, 10, 15, and 20 mg/L of phosphate solutions. Results suggest that alginate beads are effective to capture nitrate and phosphate from solutions

and the type of ionic crosslink ions has a significant influence on the total absorbed amount. A maximum (94.0 ±0.1)% of phosphate could be removed using the Al^{3+}-alginate beads and (33.6±1.9)% of nitrates by the Fe^{3+}-alginate beads. Further characterization of beads by FTIR and DSC reveal the influence of ions on the nitrate and phosphate absorption capacity by the alginate beads.

Overall, this study successfully establishes the potential of polysaccharide beads to capture nutrients and improve water quality and opens a new window of opportunities to water treatment technologies.

Keywords: Biopolymers, Sodium alginate, Beads, Water purification, Nitrates, Phosphates

CHAPTER ONE: INTRODUCTION

1.1. Background

Water is one of the most valuable components on the earth for the survival of humans, animals, and plants. Clean water is important for health, household, and agricultural applications. The world's population is on a continuous rise so as water consumption. Inadequate access to clean water is one of the most pervasive issues affecting people worldwide. The continuous industrial and technological growth further demands the availability of safe water for drinking and food production. Contaminated water causes water-borne diseases as well as interferes with the aquatic ecosystem.

Proper use of water is important for enhancing crop production. Fertilizers also play a major role in this regard. However, unconsumed fertilizers by the plants result in eutrophication (high level of nutrients such as nitrate and phosphate), admixture with the runoff, in drainage systems. Especially, in the Midwestern United States, a wide application of sub-surface drainage water has been practiced during crop production, and approximately 37% of agricultural lands use tile drainage. The tile drainage causes higher infiltration of soil nutrients into the drainage water and eventually gets disposed of in the water bodies (Heathwaite and Dils 2000). The poorly tile drainage systems, in addition, facilitate the transfer of excess water from the root-zones and carry dissolved contaminants especially nitrates and phosphates (King, Williams, and Fausey 2015). The inadvertent discharge of concentrated nitrates and phosphates causes algal blooms and hypoxia in rivers, streams, and lakes, etc.(King, Williams, and Fausey 2015). The presence of excess nutrients also leads to aquatic hypoxia in the Gulf of Mexico (Ahiablame et al. 2011;

Goolsby 1999; Rabalais 2002). It further reduces oxygen level and alters aquatic food supplies, high mortality or migration of habitat, and disruption of the aquatic life cycle (Rabalais 2002). Considering the adverse impacts of contaminated water on health and the environment, the development of water treatment technologies and restoring the water quality are critical. The goal of this research is to explore and evaluate novel and cost-effective water treatment technologies.

1.2. Rationale of the research

Crop yield could be increased by adding fertilizer to the soil. However, all of the fertilizer will not be utilized by crops but gets added to water streams. EPA recommends 10 mg/L nitrate-nitrogen and 5 mg/L phosphate in water for safe consumption. Excessive amounts of nutrients (nitrogen and phosphate) in water leads to algal blooms and hypoxia with an adverse effect on the aquatic ecosystem. High concentrations of nitrates and phosphates in drinking water are associated with breathing and digestive issues, birth defects, and bladder cancer, to name a few, especially in infants and pregnant women. They can also cause the fatal blue baby syndrome, a condition that reduces an infant's blood capacity to carry oxygen (Fewtrell 2004; Greer et al. 2005). Researchers have been developing various technologies such as reverse osmosis (RO), ultrafiltration, microfiltration, and nanofiltration (Yamashita and Yamamoto-Ikemoto 2014; Li et al. 2013; Berkessa, Mereta, and Feyisa 2019; Helness and Odegaard 2001; Henderson, Greenway, and Phillips 2007; Guo, Stabnikov, and Ivanov 2010) for treating contaminated water, but such practices are less feasible in terms of production, maintenance, and post-processing. This research aims to use natural agricultural materials such as alginate to

capture nitrate and phosphate from water to improve water quality. Alginate, a marine polysaccharide, is used extensively in food applications as a viscosifying and gelling agent. It is a negatively charged polysaccharide possessing carboxylate groups (COO^-). Alginate interactions with cations result in different network structures such as beads especially with divalent ions (e.g. Fe^{2+}, Ni^{2+}, Cu^{2+}, Zn^{2+}, $Sr^{2+,}$ and Ca^{2+}) and trivalent ions (Al^{3+} and Fe^{3+}). Such beads could be used to capture water nutrients.

1.3. Hypothesis

The hypothesis of this research is that the charge balancing cations on alginate beads will interact with nitrate and phosphate and thus the alginate beads will be effective to capture excessive nutrients from the water.

1.4. Specific Objectives

The following two research objectives have been selected:

1. To prepare and characterize alginate beads in the presence of various cross-linking divalent and trivalent ions.

2. To establish the kinetics of nutrient uptake by the alginate beads and characterize the nutrient-loaded beads.

CHAPTER TWO: LITERATURE REVIEW

Subsurface agricultural drainage allows large gains in agricultural productivity. However, nitrogen leaching from plant root-zone to drainage water demands nitrogen fertilizers which intensify the nitrate concentration in the nearby water bodies (Dinnes 2002; Keeney 2008) (Figure 1**)**. For example, continuous corn production increases the nitrate concentration in the water stream (Bakhsh A. 2007). Nitrate presence degrades water quality due to its high solubility and mobility in soils (Keeney 2008). Nitrate-nitrogen concentrations, ironically, in subsurface drainage water often exceed EPA standard of 10 mg/L. Utilization of cost-effective and renewable technologies to remove excess pollutants from sub-surface drainage water is only a viable approach.

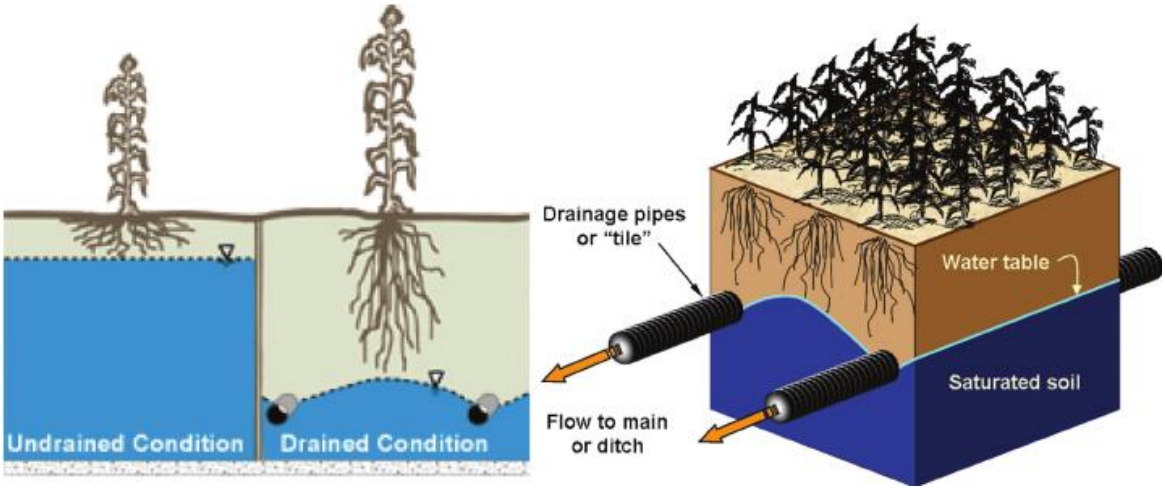

Figure 1: Drainage system and potential route for the infiltration of nutrients (e.g. nitrate and phosphate) in the drainage water. Reproduced from Blann et al. 2009.

2.1. Nitrate contamination: sources and impacts

Nitrate is an essential nutrient for plant growth. However, the discharge of excess nitrogen in tile drainage systems typically occurs through diffusion from root-zones (Figure

2**)**. Every year more and more nitrogen discharge into drainage water takes place and eventually gets disposed in nearby water bodies (river, lakes, stream, etc.). High concentration of nitrogen causes algal blooms, hypoxic aquatic environment, and disrupts aquatic ecosystems (Figure 2**)**. Several strategies such as development of nitrogen trapping systems and land management approaches have been used to reduce the nitrogen load in aquatic ecosystems (Sims 1995; Drury et al. 1996; Dinnes 2002).

2.2. Phosphate contamination: Sources and impacts

Phosphorus mainly exists as phosphate (PO_4^{3-}) and found as orthophosphate, polyphosphate, and organic phosphate in water. The agricultural fertilizer usually utilizes orthophosphate and thereby carried over to the nearby water bodies. Phosphates can also be introduced from various consumer products such as baking powders cured meats, evaporated milk, soft drinks, processed cheeses, pharmaceuticals, and water softeners (Kohler 2001). Although there are multiple points and non-point sources of phosphates, installation of tile drainage is reported to be the major source of Phosphorus load in watersheds (Figure 2**)**. The level of phosphorus in tile drainage is also dependent on soil characteristics, agricultural management, cropping system, weather, and others. The phosphorus load in the tile drainage system can exist as dissolved and particulate form. A compilation of 400 studies in 2015 on the dissolved phosphorus in drainage water in different states of USA suggests a high average concentration of 0.1 to 0.9 kg/ha/yr in dry and wet years, along with a total phosphorous load of 0.5 to 3.0 kg/ha/yr (Moore 2016).

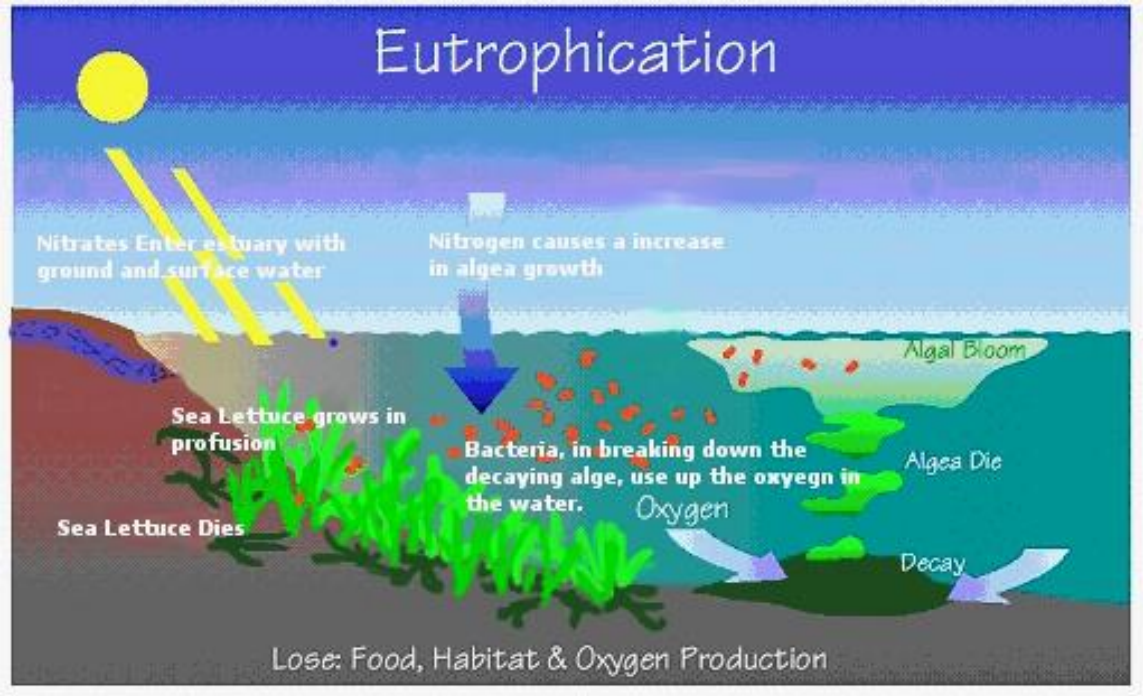

Figure 2: Eutrophication and impact of excess dissolved nitrates and phosphates in water bodies. Reproduced from http://www.wheatleyriver.ca/media/nitrates-and-their-effect-on-water-quality-a-quick-study/

2.3. Technological advancements in reducing nitrogen and phosphate loads

A high concentration of nitrate and phosphate cause eutrophication (excess growth of algae and plants), harm the ecosystem, hazardous to animals and wildlife, lack of water for agricultural and human use. The phosphate toxicity includes impaired renal function, rhabdomyolysis, and tumor lysis syndrome, and health problems associated with excess nitrate include methemoglobinemia, gastric cancer, and non-Hodgkin's lymphoma (APHA 1998). Considering the harmful impacts of nitrate and phosphate, WHO limits 5 mg/L phosphate and 10 mg/L nitrate as safe for drinking water (WHO 1985). Removal of excess nitrate and phosphate from contaminated drainage water is of immediate need.

Biological and chemical denitrification, reverse osmosis, ion exchange, electrodialysis are traditionally tested methods for the removal of nitrogen and phosphate from contaminated water (Figure 3). However, the cost of improving water quality, residual handling, and post-treatment expenses are the major hurdles of these protocols (Ranjan 2016).

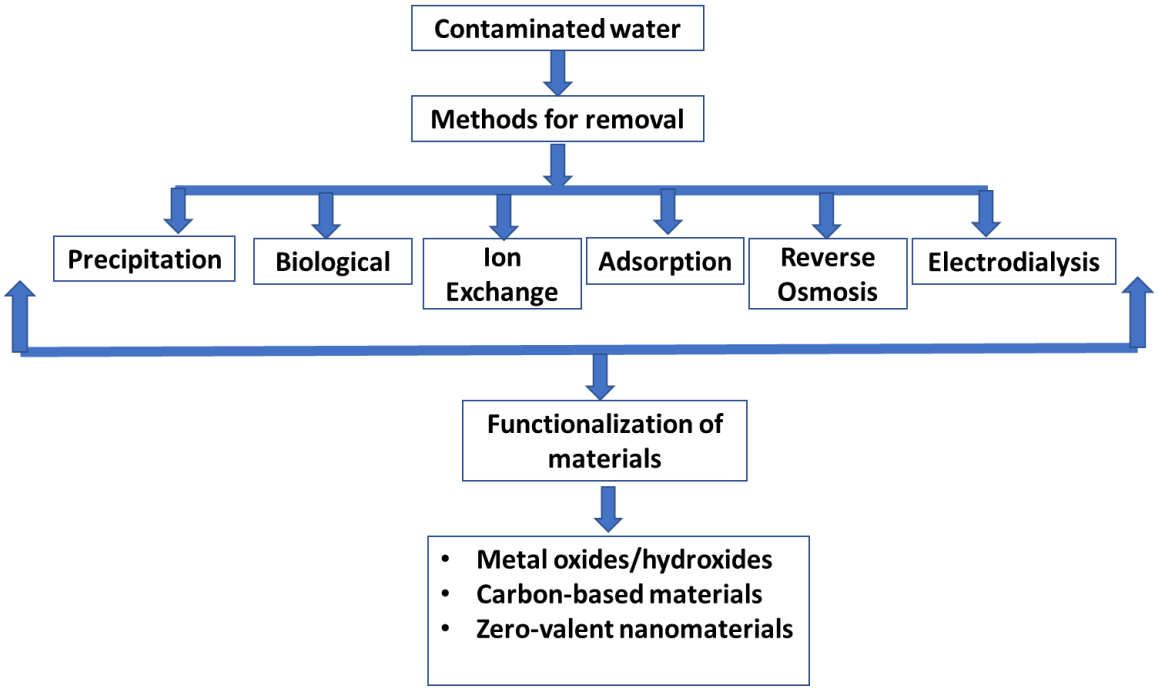

Figure 3: Traditional technologies for the removal of nitrate and phosphate from contaminated water. Adapted from Ranjan 2016.

2.3.1. The chemical methods

The chemical methods mainly use techniques such as chemical precipitation, $MgNH_4PO_4.6H_2O$ (MAP) precipitation, and electrocoagulation. Chemical precipitation is found to be less effective, however, compared to coagulation in terms of simplicity, fast operation, reduced sludge production, and operation cost. On the other hand, electrocoagulation uses electric current on electrodes (iron or aluminum) leading to coagulation of dissolved contaminants and converts them to gas bubbles (Kim 2002a; Kim 2007; Xiong 2001) (Figure 4). It involves three major steps, i) anodal oxidation, ii) destabilization of contaminants or emulsion breaking and iii) caking of unstable particles. The sedimented particles with contaminants would be removed later. This method could be effective to remove nitrates and phosphates from contaminated water (El-Naas 2009), however, removal efficiency is dependent on the pH and total dissolved solids in wastewater, and hence large-scale applicability is quite limited.

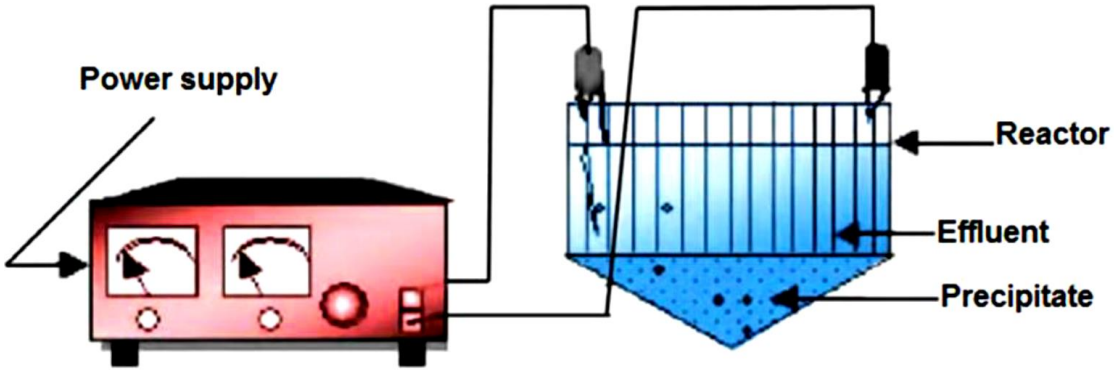

Figure 4: Schematic diagram for the electrocoagulation pilot plant (Malakootian 2009).

Chemical precipitation is also widely used to remove phosphate from wastewater, which employs multivalent metal ions such as calcium, aluminum, and iron (Tchobanoglous 2003). The use of calcium ions is usually started with applying lime ($Ca(OH)_2$) that increases the pH of wastewater by producing $Ca(CO_3)_2$ precipitate. With the increase of pH>10, the excess dissolved Ca^{2+} ions interact with dissolved phosphate ions producing hydroxylapatite precipitate.

$10\ Ca^{2+} + 6\ PO_4^{3-} + 2OH^- \leftrightarrow Ca_{10}(PO_4)*6(OH)_2$

Following a similar mechanism, removal of phosphorus can also be achieved by using iron and aluminum ions. A steady-state phosphate removal efficiency was observed upon achieving optimal removal at 85-90% (Sarparastzadeh 2007). Chemical precipitation effectively removes ortho-phosphates and particulate phosphate but with limited efficiency of polyphosphate and organic phosphorus (Maurer 1999).

The use of struvite ($Mg.NH_4PO_4.6H_2O$) has also been explored for the treatment of various types of wastewaters. This process uses combined removal of ammonium (NH^{4+}), phosphate (PO_4^{3-}), and magnesium (Mg^{2+}) from supersaturated solutions followed by the

production of MAP as a byproduct. In this process, ammonium chloride, and magnesium chloride or magnesium sulfate usually added as a source for ammonium (NH_4^+) and magnesium (Mg_2^+) that interact with dissolved PO_4^{3-} to form MAP precipitate. Struvite ($Mg.NH_4PO_4.6H_2O$) was found to produce an equal molar ratio of $Mg:NH_4:PO_4$ (1:1:1) (Gunay 2008). However, the overall mechanism is limited to pH and the optimum pH should be around 5-6. Furthermore, the process is also sensitive to water temperature and may not be applicable in different regions of the world with variable water temperature.

The physicochemical process involves the use of polymer hydrogels and crystallization using coal fly ash. Due to the presence of high content of alumina and silica, coal fly ash has been used as the adsorbent for inorganic and organic phosphates from contaminated water. The coal fly ash simultaneously acts as calcium ion supplier, pH controller, and seed crystal upon dispersing into phosphate contaminated water leading to precipitation of calcium phosphate and phosphate adsorption on the surface of the fly ash. In general, phosphate removal efficiency is dependent on the pH and CaO content in coal fly ash. However, these methods are more complex, time-consuming, and are not environmentally friendly.

While conventional adsorbents such as clay minerals, zirconia, titania, polymeric ligand exchangers and activated alumina have limited feasibility in practical water treatment application, the use of polymer hydrogels has been characterized as an effective adsorbent for large water bodies. This is attributed to the hydrophilic but large polymer network which prevents them to dissolve in water while working as adsorbent (Kioussis

2005). For example, polyallylamine hydrochloride (PAA.HCl) which chemically cross-link by the pendent amine groups (NH_2) (Kioussis 2000). The counter ions (anions) present in water to be treated interact with the pendent amine group and neutralization of free NH_2 groups. However, defects such as polymer dangling end, elastically ineffective loops, and aggregated cross-link structure, cross-linking density, topological microstructure influence the swelling properties of the polymer hydrogels and mechanical properties (Kioussis 2000).

2.3.2. The biological methods

A combination of biological and chemical methods known as bio-electrochemical denitrification is also being pursued for the removal of nitrates and phosphates from water. The natural denitrification process involves the respiratory process known as facultative anaerobes in absence of oxygen (Van Rijn 2006). The process of conversion of nitrate into nitrogen gas is mediated by denitrifying bacteria available in nature (Prosnansky 2002; Szekeres 2001). Naturally, there are two different types of de-nitrifiers available: i) heterotrophs and ii) autotrophs. Heterotrophs require carbon which usually utilizes carbohydrates for their energy source and development while autotrophs use inorganic substances for the same purpose and use of CO_2 gas as a carbon source. The rate of the denitrification process is dependent on the type of carbon source, the concentration of carbon, and the C/N ratio (Galvez 2003; Gomez 2003). Although this is a natural and cost-effective process, there are some disadvantages in the heterotrophic denitrification process such as i) some of the carbon sources are toxic and require post-treatment of the build-up byproducts, ii) poor C/N ratio causes inadequate denitrification, iii) higher C/N ratio leads

to nitrite deposition or nitrous production and iv) require a longer time for the removal of nitrates in highly concentrated wastewater (Shrimali 2001; Kim 2002b; Foglar 2005). In contrast, the autotrophic denitrification process uses CO_2 gas as carbon source and devoid of converting toxic byproducts, low biomass deposition, and less sludge production providing easier post-treatment (Shrimali 2001; Van Rijn 2006). Water electrolysis in combination with enzymatic denitrification is the main mechanism of bio-electrical denitrification (Figure 5**)**. The electrochemical method produces hydrogen in the cathode which acts as an electron donor in the conversion process of nitrates to N_2 gas (Zhang 2005). The bio-electro reactors or bioreactors stabilizes the denitrifying bacteria on the surface of the cathode and provide direct contact with the electron donor (hydrogen) and accelerate the denitrification process (Park 2005). The overall mechanism of the bio-electrochemical method can be expressed as follows:

$$2NO^{3-} + H_2O \rightarrow N_2 + 2.5\ O_2 + 2\ OH^-$$

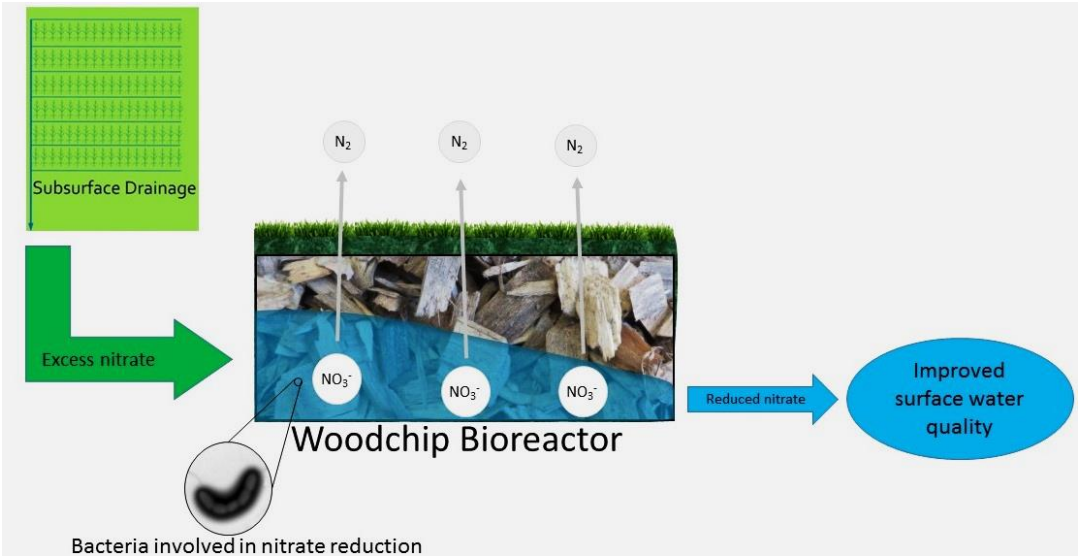

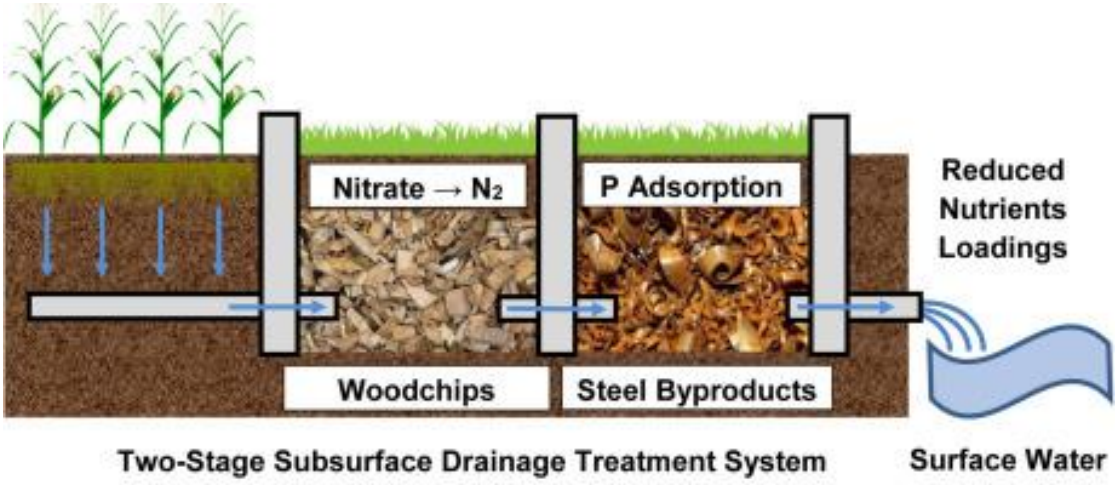

Figure 5: Typical woodchip bioreactor for denitrification and improving water quality. Reproduced from Hua et al. 2016, and https://www.egr.msu.edu/bae/water/woodchip-bioreactor.

The efficiency of bioreactors is influenced by materials, shape, the number of electrodes, and overall design. Carbon source such as granular activated carbon (GAC) and graphite has been used along with metals such as stainless steel, titanium, and copper (Mousavi 2011).

Among other woodchip bioreactors, a newly developed strategy for the removal of nitrates from drainage water uses a bio-electrochemical denitrification process (Figure 5**)**. Woodchip bioreactors made by a buried trench filled with woodchips and routing the drainage water through bioreactors. A woodchip bioreactor can reduce annual nitrate load from 10-90% based on the type of bioreactor, drainage system, and weather patterns. Hua *et al.* (2016) investigated the nitrate and phosphate removal efficiency from subsurface drainage water using laboratory woodchip bioreactors connected with steel byproduct filter (Figure 5) (Hua et al. 2016). These bioreactors showed nitrate removal efficiency of 53.5 to 100% with a removal rate of 10.1–21.6 g $N/m^3/d$, while phosphate removal capacity was found to be 3.7 mg phosphate per gram (Hua et al. 2016). Although woodchip bioreactors are viable, they carry few side effects of producing and accumulating toxic methyl mercury. This process becomes activated with the storage of water in the bioreactors for a longer time after the removal of nitrates. One important process is the conversion of sulfide to hydrogen sulfide gas. The bacteria that involve in denitrification can also convert the mercury present in water to toxic methyl mercury. Regular monitoring of the bioreactors during the low-flow period can eliminate this concern. Another concern related to the denitrification process is the production of nitrous oxide which is the greenhouse gas. Research efforts still being pursued to minimize the production of nitrous oxide in

bioreactors. Table 1 highlights the comparison of different strategies of nitrate and phosphate removal.

Table 1: Comparison of nitrate and phosphate removal strategies

Methods	Materials	Target nutrients	Advantages	Disadvantages
Chemical precipitation	Metal salts (Al and Fe salts)	Phosphate	Low cost	More sludge production, less environment friendly
MAP precipitation	NH_4Cl, $Na_3(PO_4)$ and $MgSO_4$ or $MgCl_2$	Phosphate	Low cost	More sludge production, less environment friendly
Electrocoagulation	Al and Fe electrodes	Phosphate and nitrate	Less sludge production, environment-friendly, simple, faster	Higher cost
Physicochemical	PAA.HCl gels, Coal fly ash	Phosphate	Less sludge production, environment friendly, low cost	More complex, time-consuming
Bio-electrochemical method	Coated graphite, granular activated carbon, woodchips	Nitrate and phosphate	Low biomass deposition, and less sludge production	Toxic byproducts

2.4. Biopolymers for the treatment of water

Biopolymers have attracted researchers for the development of cost-effective and safe water treatment technologies. Their structure, physiochemical properties, solubility, stability, and reactive functional groups are attractive for water treatment applications. The most widely studied of them include chitin, starch, and their derivatives chitosan and cyclodextrin. Chitin is the most abundant natural polymer obtained as a byproduct for seafood processing. It is a mucopolysaccharide with α, β-1,4-linkage. Since shrimp, lobster, and crab shells are abundantly available, chitosan (deacetylated derivative of chitin) can be produced at a low cost. Similarly, starch is another abundant biopolymer that contains two polyglucans, amylose and amylopectin. Its derivative cyclodextrin contains six to twelve glucose units. Modification of these biopolymers with different cross-linking agents can provide macromolecular superstructures such as gels, hydrogel networks, beads, membranes, fibers, films, and composites. A couple of cross-linking agents that are commonly used include glutaraldehyde, benzoquinone, epichlorohydrin, ethylene glycol diglycidyl ether, phosphorus oxychloride, and carboxylic acids etc. Table 2 highlights a few of the tests biopolymers-based water treatment technologies for the removal of different water pollutants.

Table 2: Utilization of biopolymers for the development of water treatment technologies

Biopolymer	Cross-linking agent	Types of product	Removal of ions
Chitosan	GLA	Beads	Ni^{2+}, Cu^{2+}, Zn^{2+}, Pd^{2+}
	EPI	Beads	Dyes
	GLA	Membranes	Ni^{2+}, Cu^{2+}
	Benzoquinone	Beads	Cu^{2+}, Zn^{2+}
	GLA, EGDE	Beads	Dyes
	EPI, GLA, EGDE	Beads	Cu^{2+}
Starch	EPI	Gels	Phenols
	EPI	Gels	Dyes
	EPI	Beads	Dyes
	$POCl_3$	Beads	Pb^{2+}, Cu^{2+}, Cd^{2+}
Cyclodextrin	EPI	Beads	Organics
	EPI	Beads	Bile acids
	EPI	Gels	Organics
	EPI	Gels	Phenols
	EPI	Gels	B-naphthol
	EPI	Gels	Dyes

GLA: Glutaraldehyde; EPI: Epichlorohydrin; EGDE: Ethylene glycol diglycidyl ether;

2.5. Advantages of using biopolymers for the development of water treatment technologies

Generally, a suitable water treatment technology should fulfill the following requirements,

a) Efficient for the removal of contaminants

b) High adsorption capacity and rate of adsorption

c) Selectivity for a contaminant

d) High adsorption surface area

e) High physical strength and stability

f) Renewability/reusability

g) Effective in a wide range of wastewater

h) Low cost

Biopolymers are cost-effective, highly efficient, stable, versatile, and easy to regenerate as compared to synthetic materials.

2.6. Fabrication of alginate for the removal of nutrients from contaminated water

Alginate is a natural, biocompatible, biodegradable, and economical polymer obtained from renewable marine source brown marine algae by sodium hydroxide solution treatment (KIM 1990; Patel et al. 2016). Commercially available alginate are usually isolated from *Ascophyllum nodosum*, *Macrocystis pyrifera Laminaria hyperborea*, *Laminaria digitata*, and *Laminaria japonica* (Lee and Mooney 2012; Clark 1936). Its molecular weight varies from 32,000 to 400,000 daltan (Lee and Mooney 2012). The viscosity of alginate solution is dependent on the pH of the bulk solution and reaches the maximum at pH 3.0 to 3.5 due to complete protonation of the COO^- groups and higher extent of hydrogen bonds (Lee and Mooney 2012). It is a binary linear heteropolysaccharide with β-D-mannopyranosyl uronate and α-L-glucopyranosyl uronate linked through 1→4 fashion (Arne 1967). Alginate may exist both as homopolymeric (such as polymannuronate or polyguluronate) and heteropolymeric (mixed sequences). The structure can also be expressed as M-block, G-block, and MG-block (Figure 6).

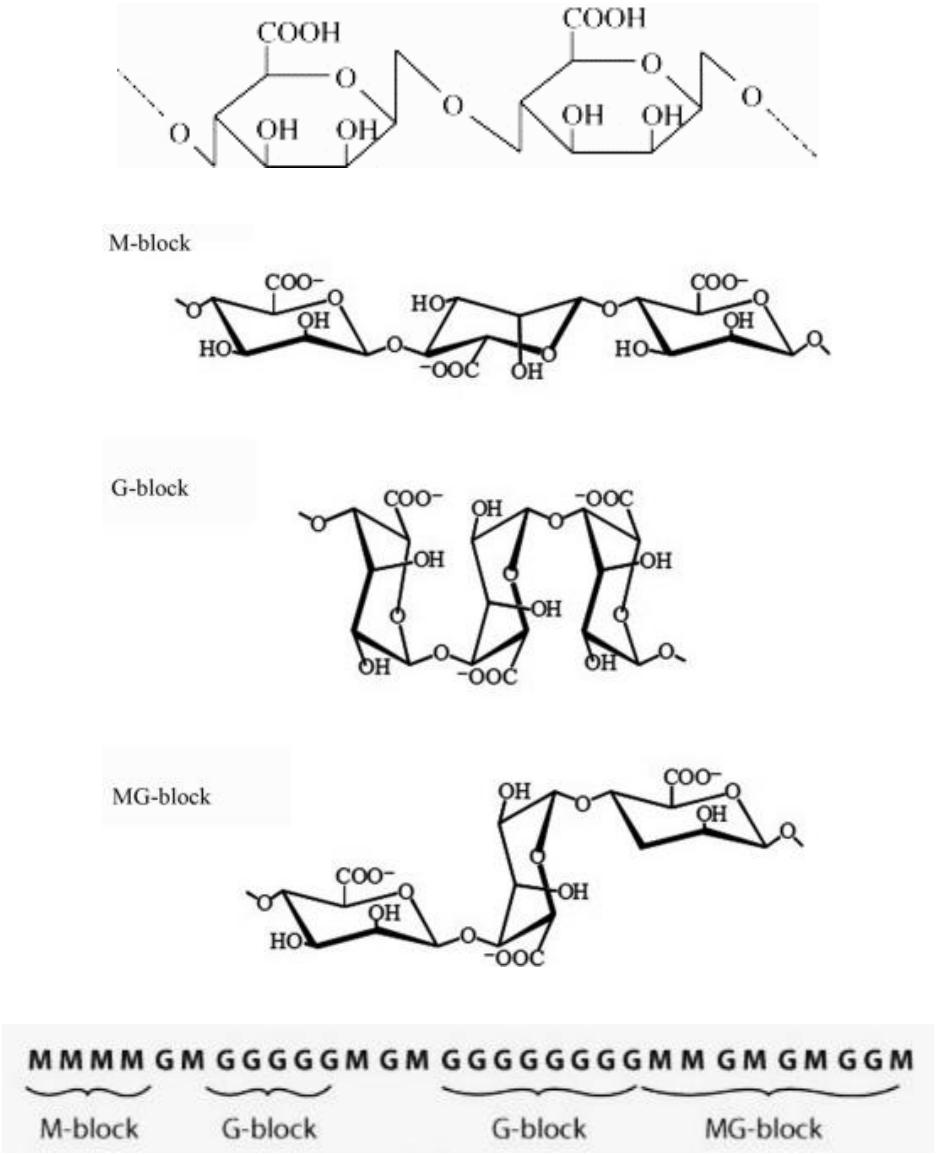

Figure 6: Chemical structure of alginate as monomer and chain or block conformation. Obtained from Soares 2004; Takeshita 2016.

Its solubility is dependent on the pH of the solvent and types of counter ions. Calcium and magnesium salt forms are insoluble in water, while sodium, potassium, and ammonium salts are water soluble (Table 3). The solubility is mainly influenced by the electrostatic charges of the uronic acid and surrounding ionic strength.

Table 3: Solubility of alginic acid and its salts in different pH conditions. Obtained from (Vijayalakshmi 2019)

Types of alginic acids	Acidic conditions	Alkaline conditions
Alginic acid	Insoluble	Soluble
Sodium alginate	Insoluble	Soluble
Potassium alginate	Insoluble	Soluble
Calcium alginate	Insoluble	Insoluble
Propylene glycol alginate	Soluble	Soluble

Alginate, as a sodium salt, is used extensively in food applications as a viscosifying, thickening gelling agent, and stabilizer (Table 4) (Zhao et al. 2010). The calcium gelled-sodium alginate has been used in beverages to improve functional properties as well as influence the gastric emptying and nutrient absorption (Torsdottir et al. 1991; Georg Jensen et al. 2012).

Table 4: Permissible limit of alginates in food products. Modified from (Vijayalakshmi 2019).

Category of food	Ammonium alginate	Calcium alginate	Potassium alginate	Sodium alginate	Propylene glycol alginate
Alcoholic beverages		0.4%			
Baked goods		0.002%			0.5%
Cheese					0.9%
Condiments and relishes				1.0%	0.6%
Confections and frostings	0.4%	0.4%	0.1%	0.3%	0.5%
Egg products		0.6%			
Fats and oils	0.5%	0.5%			1.1%
Frozen dairy desserts					0.5%
Gelatins and puddings		0.25%	0.7%	4.0%	0.6%
Gravies and sauces		0.4%	0.4%		0.5%
Hard candy				10.0%	
Jams and jellies	0.4%	0.5%			0.4%
Pimento ribbons for stuffed olives				6.0%	
Processed fruits and fruit juices			0.25%	2.0%	
Seasonings and flavors					1.7%
Sweet sauces	0.5%	0.5%			
All other food categories	0.1%	0.3%	0.01%	1.0%	0.3%

The gelling property of alginate in the presence of divalent cations (e.g. Ca^{2+}) has been widely investigated. The guluronate blocks of alginate allow a high degree of cross-linking in the presence of divalent cations forming the Egg-box model (Figure 7) of cross-linking (Grant 1973).

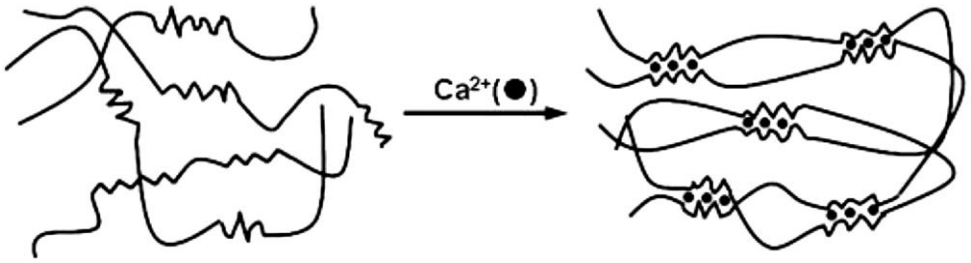

Figure 7: Ionic cross-linking of alginate (Egg-box model), formed only with guluronate blocks interstices with Ca^{2+} ions. Reproduced from Lee and Mooney 2012.

However, the feasibility of developing alginate-based beads and the ability to capture excess nutrients from contaminated water remains to be elucidated. In this regard, it is hypothesized that the availability of negatively charged carboxylate groups (COO^-) facilitates the interaction with surrounding cations result in special network structures to form beads that could be used to capture water nutrients.

CHAPTER THREE: MATERIALS AND METHODS

3.1. Materials

Highly pure and food grade sodium alginate was obtained from AIC LLC (Westborough, MA, USA). The nitrate nitrogen and phosphate standard solutions were purchased from HACH, (Loveland, Colorado, USA). Aluminum chloride, ferric chloride, ferrous chloride, copper chloride, zinc chloride, strontium chloride, calcium chloride, and nickel chloride were obtained from Sigma-Aldrich (St. Louis, MO). Distilled water was used as a solvent.

3.2. Methods

3.2.1. Preparation of alginate solution

An appropriate amount of Sodium alginate powder was added slowly to the boiled distilled water to prepare 2% (w/v) solution. The prepared solution was kept heating at 95-100 ºC and stirring overnight at 600-700 rpm. The solution was made sure to be homogeneous without any powder particles before moving forward with beads preparation.

3.2.2. Preparation of cationic salt solution

Different stock salt solutions (divalent and trivalent cations) were freshly prepared separately using distilled water. The divalent and trivalent cationic salts that were screened for the preparation of alginate beads with target specifications were Fe^{2+}, Cu^{2+}, Ca^{2+}, Zn^{2+}, Ni^{2+}, Sr^{2+}, $Fe^{3+,}$ and Al^{3+}. Briefly, a 3% (w/v) salt solution was prepared at room

temperature. The required weight of salt crystals was dissolved in distilled water under constant stirring to make a clear solution. The homogeneity of the solution was confirmed by visual observation and without visible particle or precipitation.

3.2.3. Preparation of alginate beads

To avoid interference of contaminated ions, all experiments were conducted with distilled water. The alginate solutions were loaded into a disposable 5 mL syringe fitted with 20-gauge hypodermic needle. Then the solution was added dropwise into each 3% (w/v) cationic salt solutions and monitored for coagulation to form alginate beads (Figure 8). The droplet size and rate of addition were optimized to ensure the formation of beads with uniform sizes. The resulting beads were left into their respective salt solution overnight to allow complete cross-linking and forming stable beads. The beads were then filtered out and dried in room temperature to use for characterization and further evaluation for the removal of nutrients from contaminated water.

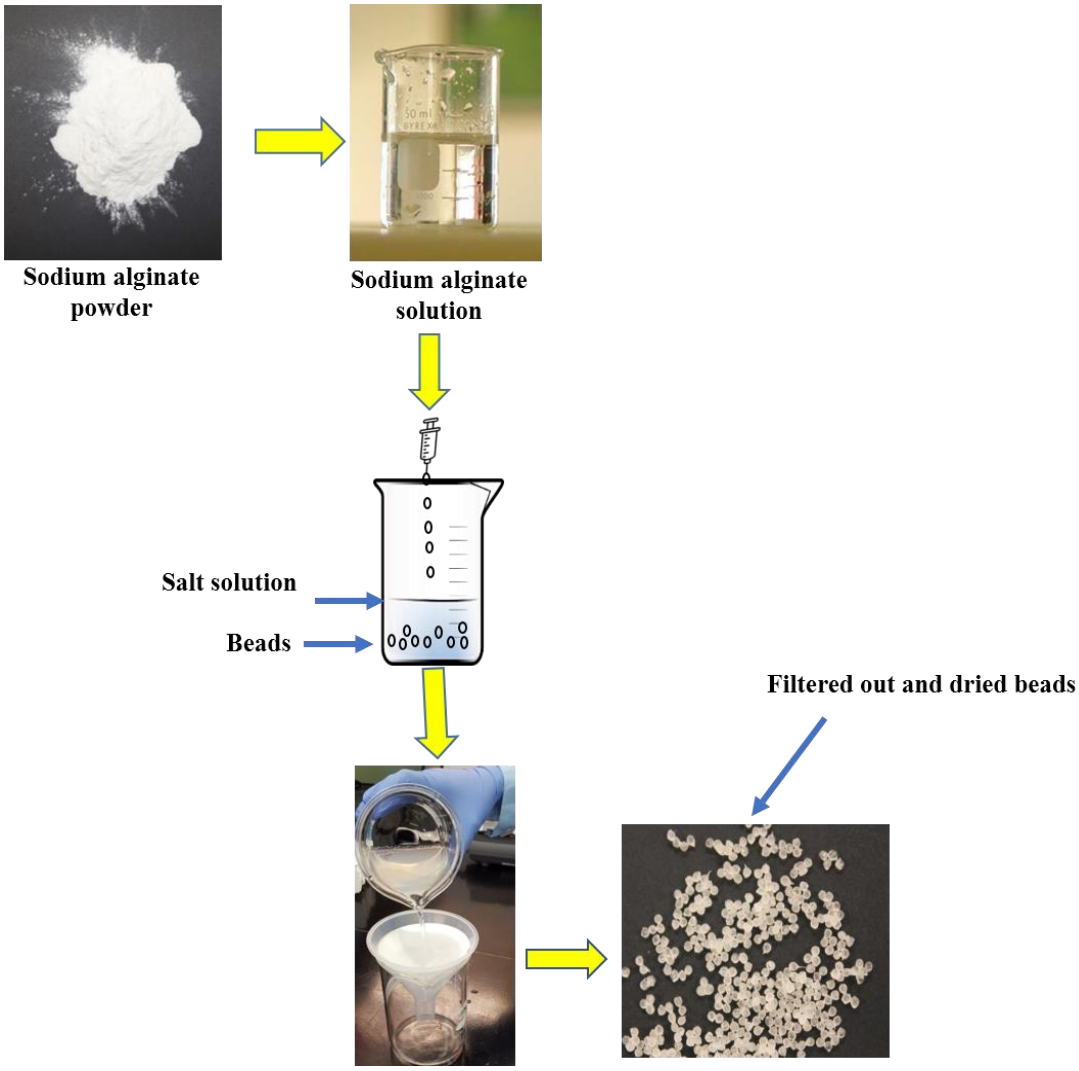

Figure 8: Schematic diagram for the preparation of beads.

3.2.4. Physical characterization of the beads

The beads formed with different cations were visually observed for the appearance, uniformity in size, color, shape, and strength. Any sub-optimal beads with variable sizes, shape, and soft nature were discarded from the study.

3.2.5. Removal of nitrate and phosphate from standard water

The screening of different alginate beads was conducted using standard nitrate and phosphate solution. The absorption efficiency was evaluated at different concentrations of nitrate and phosphate. The phosphate absorption efficiency was determined by using 1, 5, 10, 15, and 20 mg/L solutions. Similarly, nitrate absorption efficiency was determined by using 5, 10, and 25 mg/L solutions. Briefly, in a 250 mL glass beaker, 100 mL of nitrate or phosphate standard solution was added, at room temperature, along with 300 mg of alginate beads. A terminal sampling method was used to collect water samples for each time point using individually prepared standard solutions. The water samples were collected at different time points for up to 24 hours. At the end of each time point, the collected water samples were immediately stored at -20 ^{o}C until further experiment. A proposed schematic diagram for the absorption of nitrate or phosphate is presented in Figure 9.

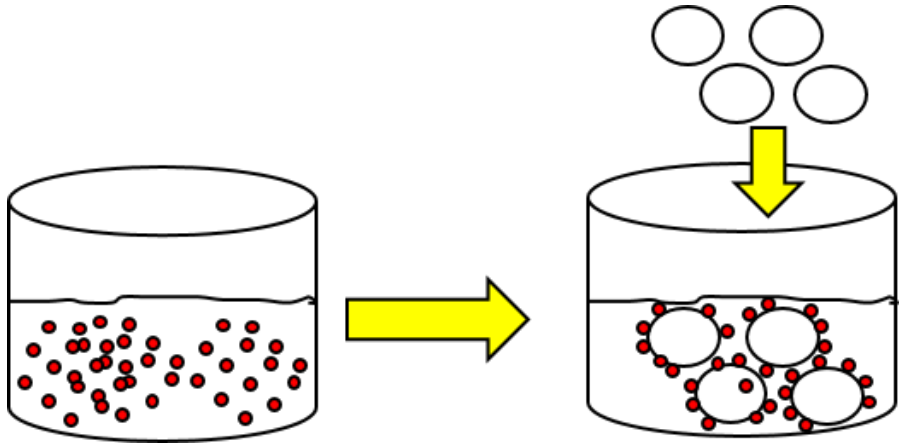

Figure 9: Schematic representation of the removal of nitrate and phosphate from water. The empty circle represents alginate beads and red circle represents nitrates/phosphates in water.

AQ2 analyzer was used to detect the nitrate and phosphate amount in the water. The concentration of each nitrate or phosphate samples at each time point were analyzed in duplicate. The percent absorption of nitrate or phosphate was calculated based on the reduction of the concentration at each time point as follows:

$$\%\text{Absorption} = \frac{(C_0 - C_t) * 100}{C_0}$$

Where, C_0 is the initial concentration of nitrate or phosphate standard water

C_t is the concentration of nitrate or phosphate at time point t.

The mean values have been reported. The alginate beads without any absorption of nitrate or phosphate were not considered for further characterization and are not presented for comparison.

3.2.6. Chemical characterization of the beads

To understand any textural differences among the beads before and after the uptake of nitrate and phosphorus the following two characterizations were performed.

3.2.6.1. Differential Scanning Calorimetry (DSC)

Thermal analysis of the ground beads with and without nutrients were performed using TA Q1000 differential scanning calorimeter (TA Instruments, New Castle, Delaware). T-zero Hermetic aluminum sample pans were used to load approximately 3.0 mg sample and sealed with T-zero hermetic lids using the hermetic press (TA Instruments). As a reference, an empty aluminum pan was used. To purge the sample chamber an ultra-high purity nitrogen gas (40 mL/min) was used. The range of temperature and heating rate were used as 20 to 250 °C and 10°C/min, respectively. The mean values from duplicated quantifications are reported.

3.2.6.2. Attenuated total reflectance-FTIR spectroscopy (ATR-FTIR)

Identification of functional groups of the alginate beads with and without nutrients were performed using a Nicolet Avatar 360 ATR-FTIR spectrometer (Varian, Inc., CA). All solid bead samples were ground separately into powder form to make compatible with the ATR-FTIR spectrometer. In the range of 400 to 4000 cm^{-1} each sample was scanned and EZ OMNIC software was used to collect the spectra with an average of 64 scans. Prior

to loading each sample, background spectrum was collected and was subtracted from the respective sample spectrum.

3.3. Statistical Analysis

Microsoft Excel (version 2016) and R software (version 3.4.0) were used to analyze all the data. A one-way repeated measures ANOVA and Single factor ANOVA were used to test the significance of the differences. Further Bonferroni method and Tukey's HSD (Honestly Significant Difference) test were performed for post hoc multiple comparisons. The level of significance was used as $\alpha = 0.05$. Homogeneity of variance assumption was applied to conduct the tests.

CHAPTER FOUR: RESULTS AND DISCUSSION

4.1. Optimization of alginate concentration and selection of cross-linking ions

The straightforward method to obtain alginate beads with higher mechanical stability is dependent on the concentration of the alginate solution. However, higher alginate concentration increases the viscosity of the pre-gelled solution that in-turn clogs syringe and thwarts formation of uniform size beads. Thus, 2% pre-gelled alginate solution is used in the study. A thorough screening of cross-linking agents were performed by evaluating the ability to form beads and stability of beads in water after manufacturing. The Ca^{2+} ions are widely studied for different applications of alginate, with respect to its intrinsic ability to cross-link alginate chains (Rosellini et al. 2009; Kuo and Ma 2008). However, in this study, six different divalent and two trivalent cations (Fe^{2+}, Zn^{2+}, Cu^{2+}, Ni^{2+}, Ca^{2+}, Sr^{2+}, $Al^{3+,}$ and Fe^{3+}) were screened to understand variations in the beads formation, difference in physicochemical properties, beads stability, rigidity, brittleness, and efficiency in removing nutrients from water. The ionic cross-linkers interact with carboxyl groups of glucuronic acid residues of two/three neighboring alginate chains and form a three-dimensional network (Hyun-Joon Kong 2002).

4.2. Physical characterization of alginate beads

The alginate beads were instantly formed after dropping the alginate solution into different cationic salt solutions. The optimization of the flow rate of the alginate solution, fixed concentration of cross-linking solution and fixed period of cross-linking enables the uniformity of the sizes of the beads. The appearance and color of the beads varied based

on the cationic salts used for cross-linking. Table 5 and Figure 10 highlight the color and appearance of alginate beads respectively in different salt forms.

Table 5: Color of alginate beads

Alginate beads	Color
$+Fe^{2+}$	Red brown
$+ Fe^{3+}$	Pale yellow
$+ Al^{3+}$	Off-white
$+ Cu^{2+}$	Blue
$+ Zn^{2+}$	Shiny gray
$+ Ni^{2+}$	Green
$+ Sr^{2+}$	Silvery
$+ Ca^{2+}$	Off-white

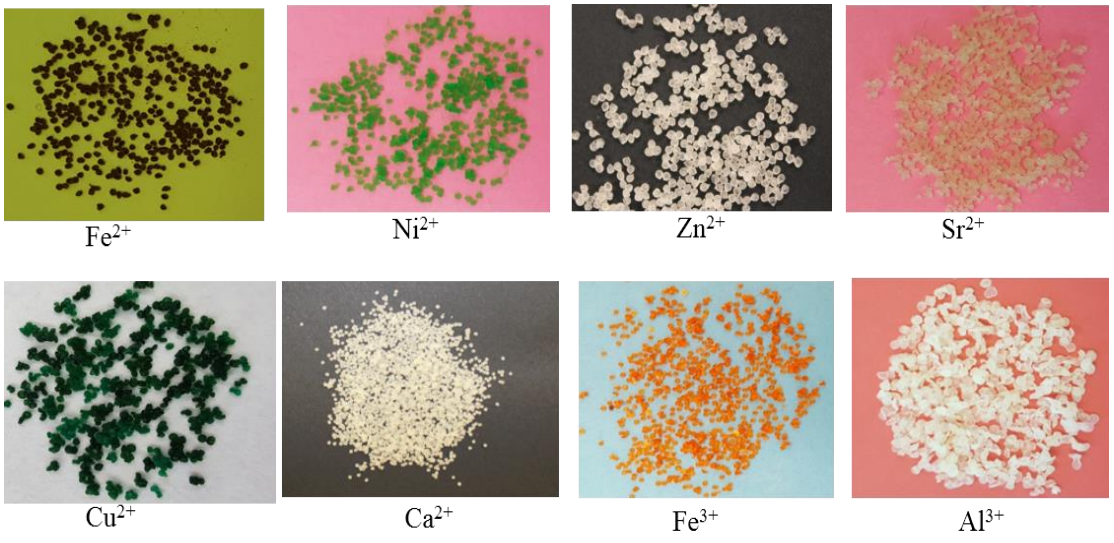

Figure 10: Appearance of alginate beads prepared by cross-linking with various cations.

4.3. Efficiency of removal of phosphate and nitrate from standard water samples

The uptake kinetics of nutrients (nitrate or phosphate) by alginate beads were studied using standard solution of nitrate and phosphate.

4.3.1. Phosphate removal

The initial screening showed that aluminum, iron, and zinc cross-linked alginate beads can absorb a detectable amount of phosphate at all concentrations and results are presented in Figure 11 through 15. The phosphate absorption increases over time and alginate-Al^{3+} beads could absorb up to (94.0±0.1) % of phosphate in 24 hours. Similarly, alginate-Fe^{2+} and alginate-Zn^{2+} beads could absorb up to (93.6 ± 1.0) % and (40.0 ± 0.2) % of phosphate, respectively, in 24 hours. The order of absorption efficiency is found to be alginate-Al^{3+} > alginate-Fe^{2+} > alginate-Zn^{2+}. Overall, the type of ionic cross-linker appears to dictate the amount of phosphate that could be absorbed by the alginate beads.

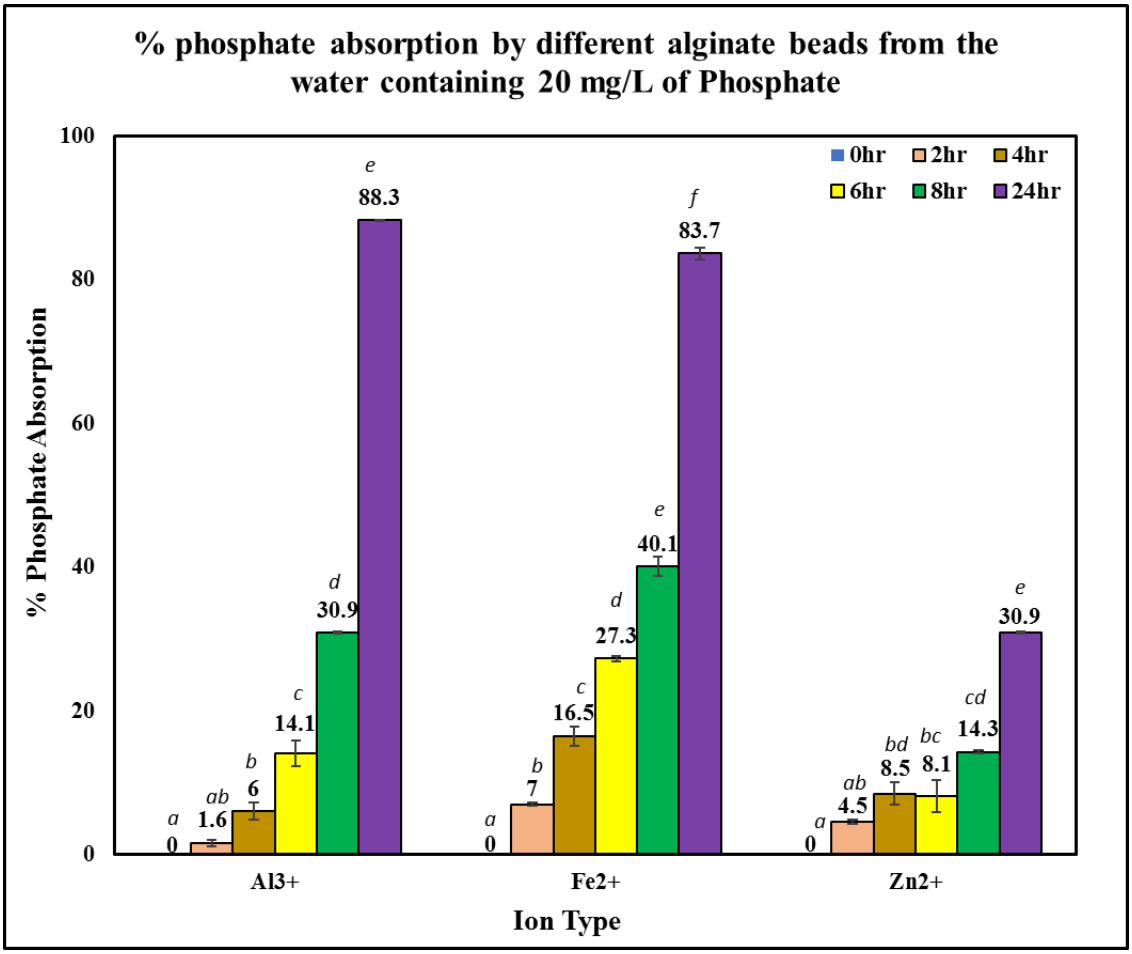

Figure 11: Percent of phosphate absorption by different alginate beads using 20 mg/L of standard phosphate water. Each bar represents mean ± SE. For each ion type, means share same letters indicate the differences are not statistically significant, while different letter indicates significantly different from each other ($p < 0.05$).

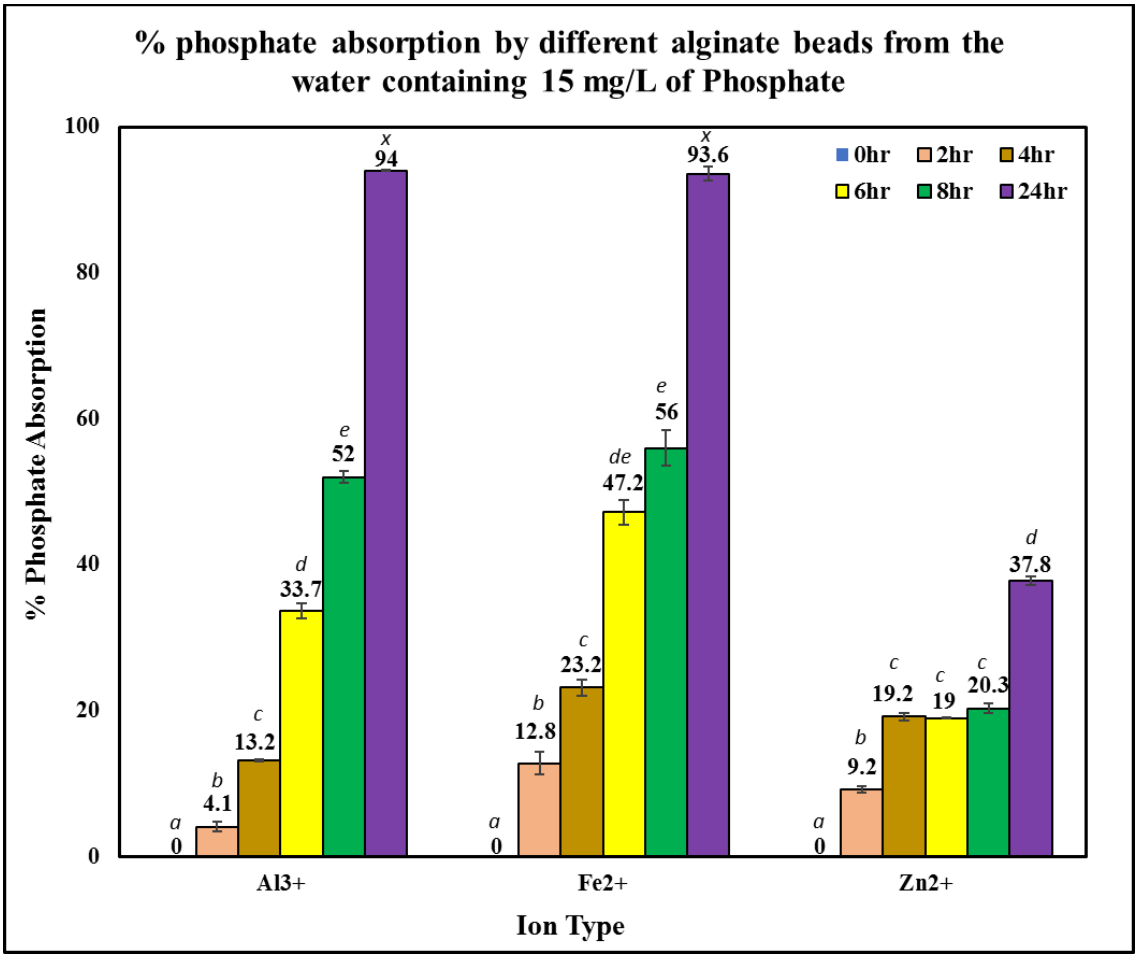

Figure 12: Percent of phosphate absorption by different alginate beads using 15 mg/L of standard phosphate water. Each bar represents mean ± SE. For each ion type, means share same letters indicate the differences are not statistically significant, while different letters indicate significantly different from each other ($p < 0.05$).

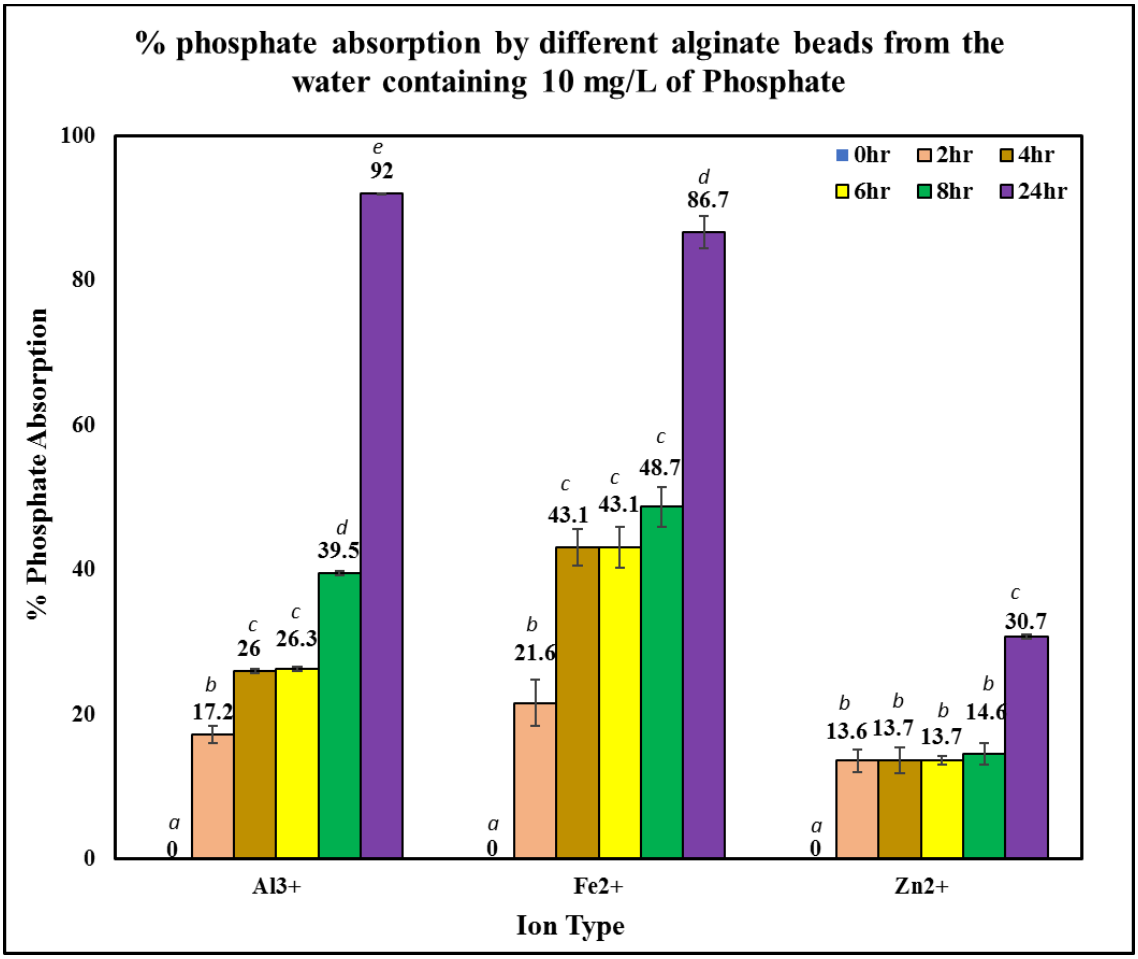

Figure 13: Percent of phosphate absorption by different alginate beads using 10 mg/L of standard phosphate water. Each bar represents mean ± SE. For each ion type, means share same letters indicate the differences are not statistically significant, while different letters indicate significantly different from each other ($p < 0.05$).

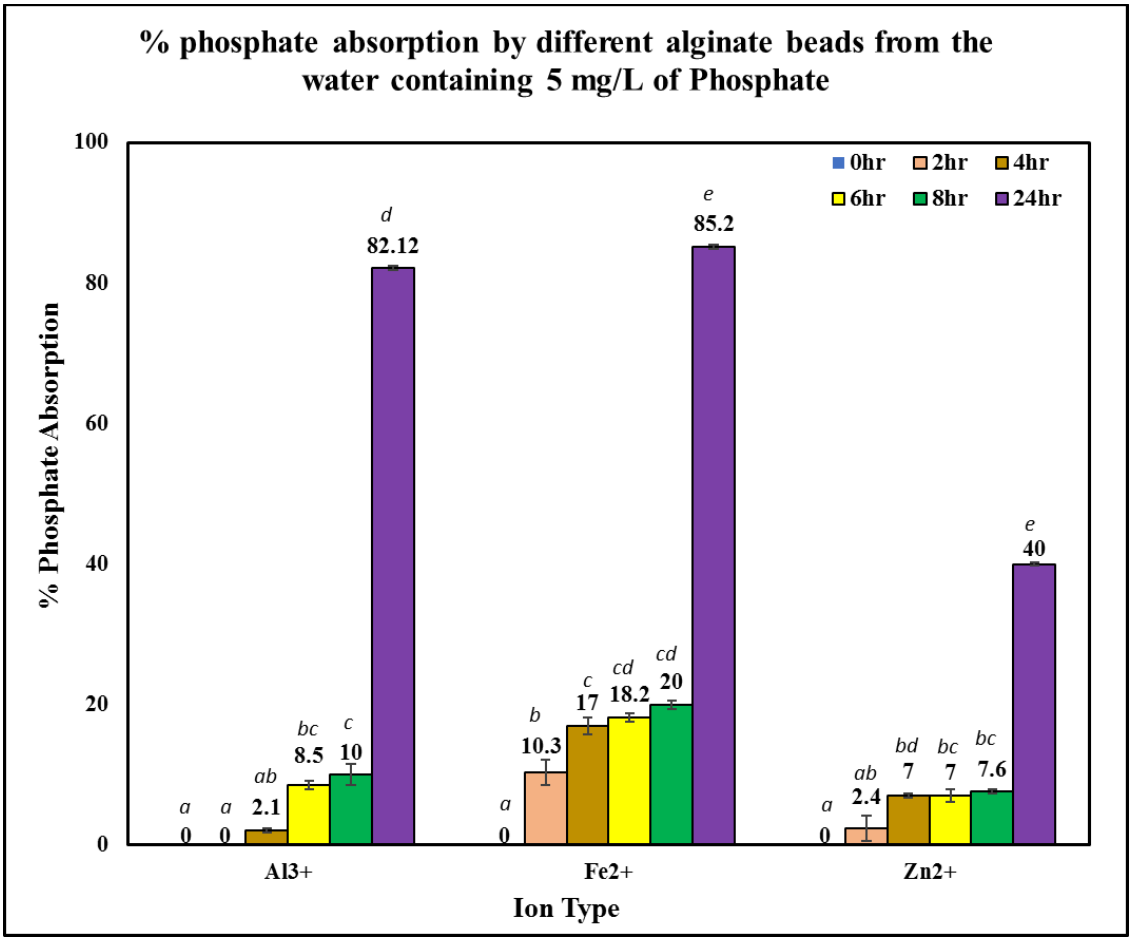

Figure 14: Percent of phosphate absorption by different alginate beads using 5 mg/L of standard phosphate water. Each bar represents mean ± SE. For each ion type, means share same letters indicate the differences are not statistically significant, while different letters indicate significantly different from each other ($p < 0.05$).

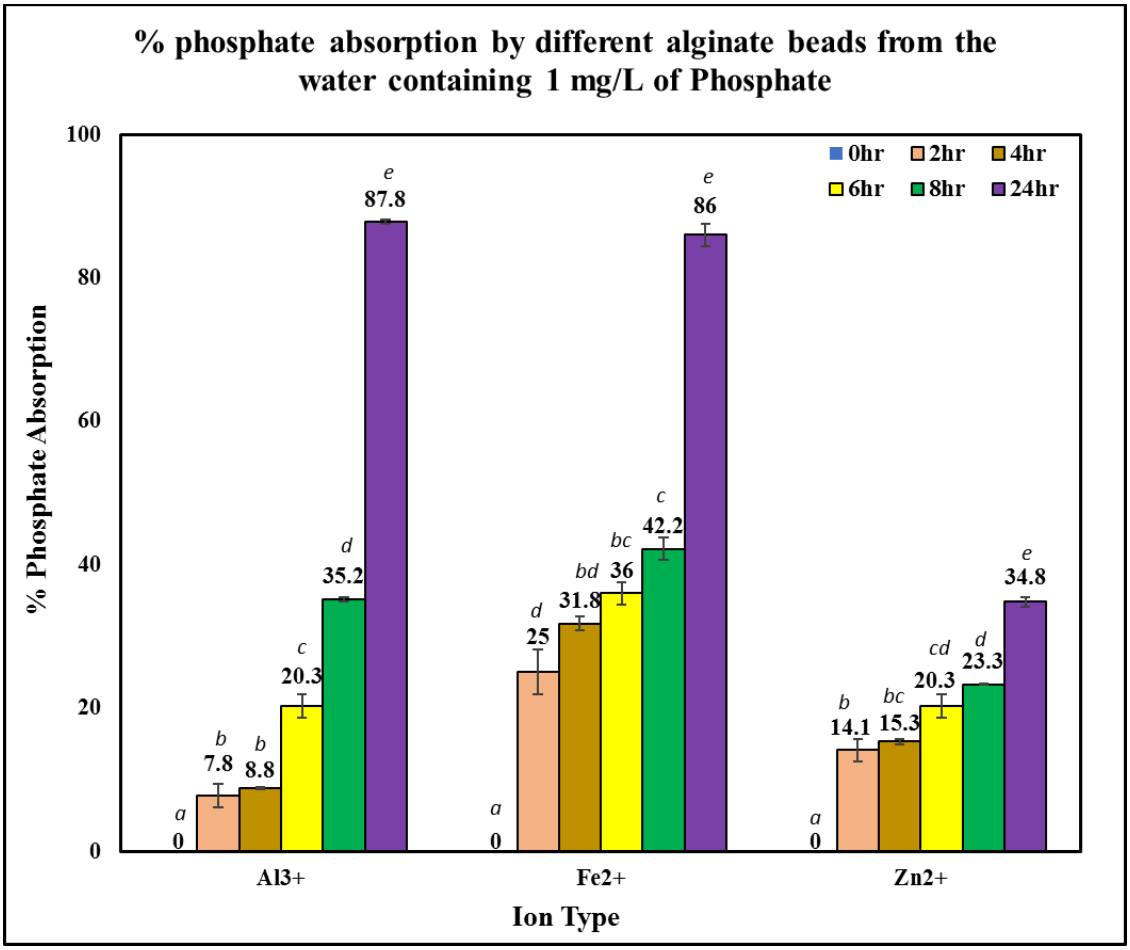

Figure 15: Percent of phosphate absorption by different alginate beads using 1 mg/L of standard phosphate water. Each bar represents mean ± SE. For each ion type, means share same letters indicate the differences are not statistically significant, while different letters indicate significantly different from each other ($p < 0.05$).

4.3.2. Nitrate removal

Although nitrate absorption has been carried for 24 hours, maximum absorption for most of the beads has been observed at 6 hours and results are presented in Figure 16 to 18. A maximum (33.6 ±1.9) % of absorption is observed by alginate-Fe^{3+} beads (Figure 16). The alginate-Al^{3+}, alginate-Fe^{2+}, alginate-Cu^{2+}, alginate-Sr^{2+}, alginate-Ni^{2+} and alginate-Zn^{2+} beads absorbed up to (25.0 ±1.4)%, (25.9± 0.6)%, (22.6 ± 0.7)%, (23.4 ±1.3)%, (12.3 ± 0.3)% and (10.4 ± 0.04)%, respectively. Overall, the peak nitrate absorption was obtained at 6 hours and a gradual decrease of nitrate absorption was detected afterwards presumably due to slow release of absorbed nitrate.

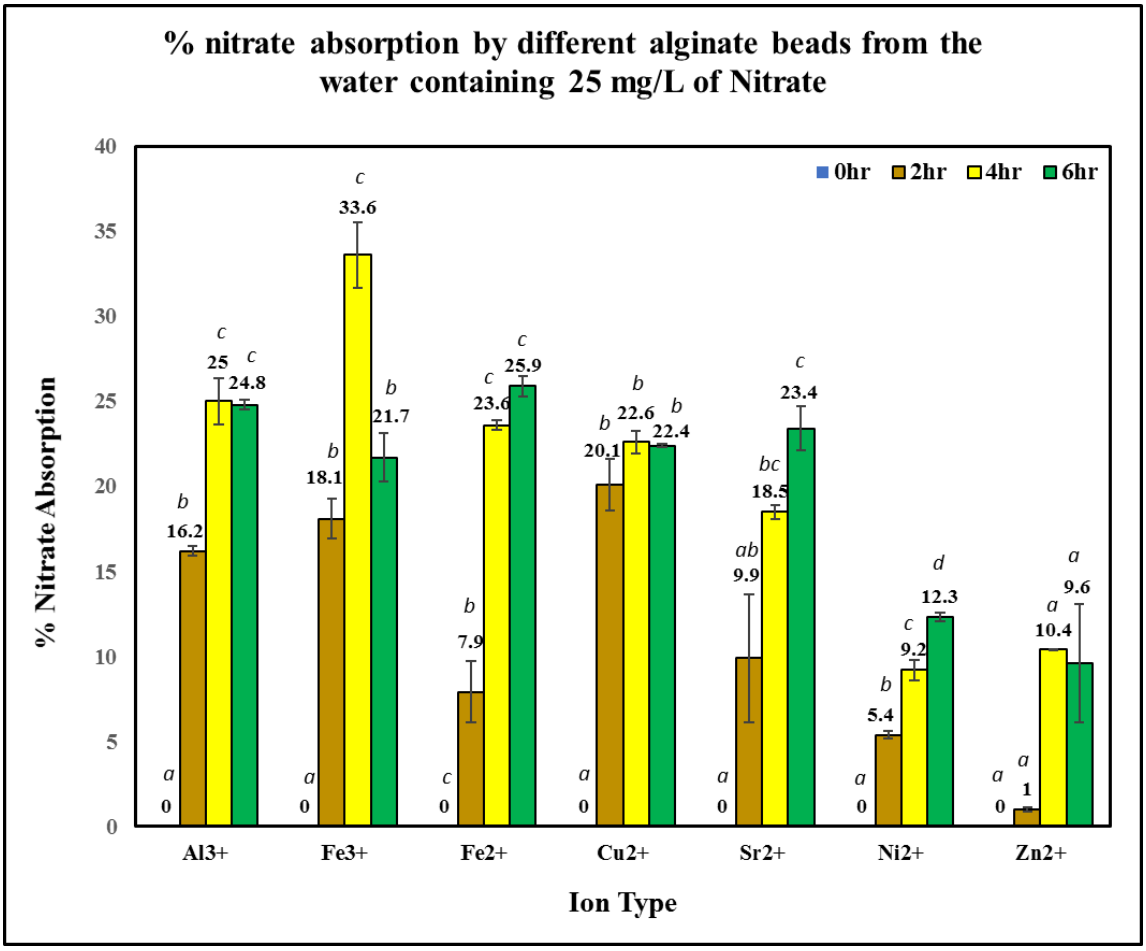

Figure 16: Percent of nitrate absorption by different alginate beads using 25 mg/L of standard nitrate water. Each bar represents mean ± SE. For each ion type, means share same letters indicate the differences are not statistically significant, while different letters indicate significantly different from each other ($p < 0.05$).

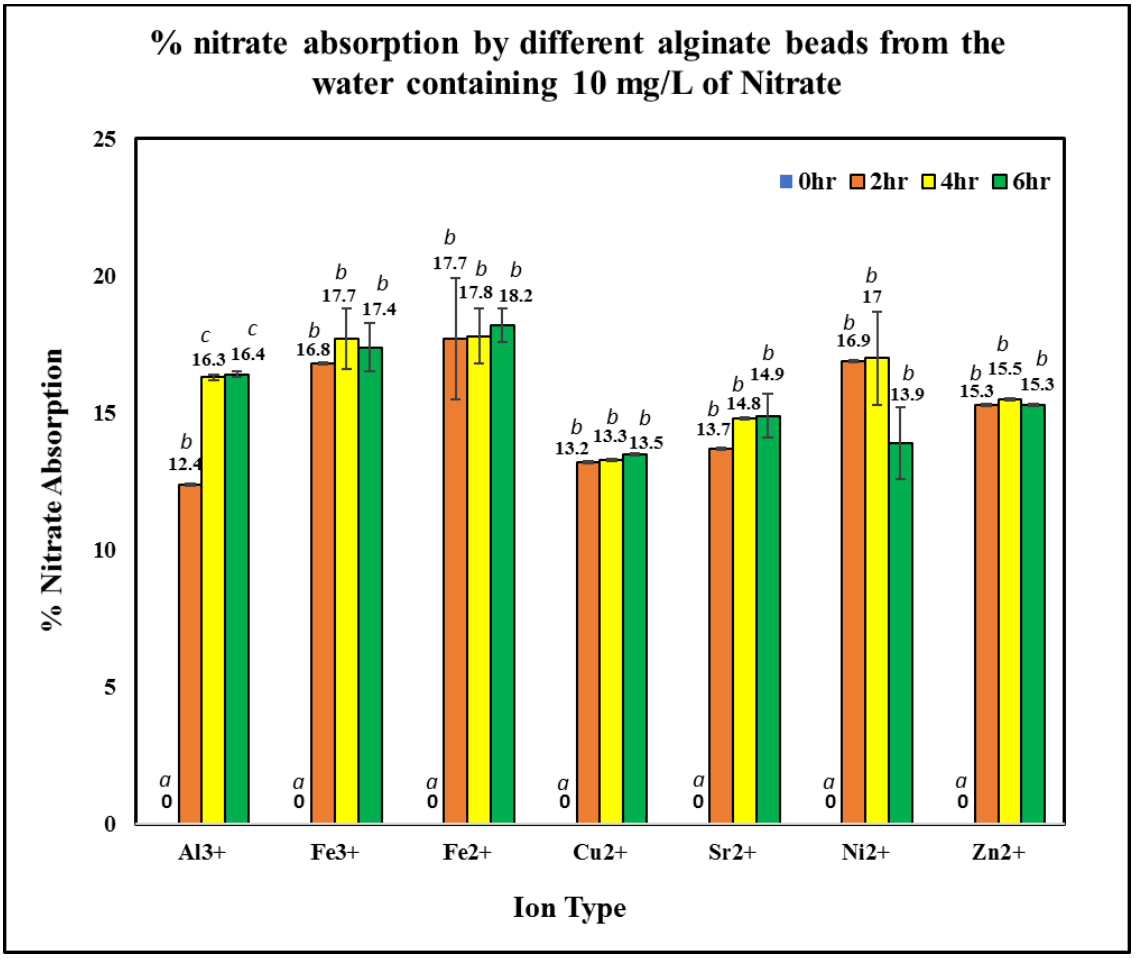

Figure 17: Percent of nitrate absorption by different alginate beads using 10 mg/L of standard nitrate water. Each bar represents mean ± SE. For each ion type, means share same letters indicate the differences are not statistically significant, while different letters indicate significantly different from each other ($p < 0.05$).

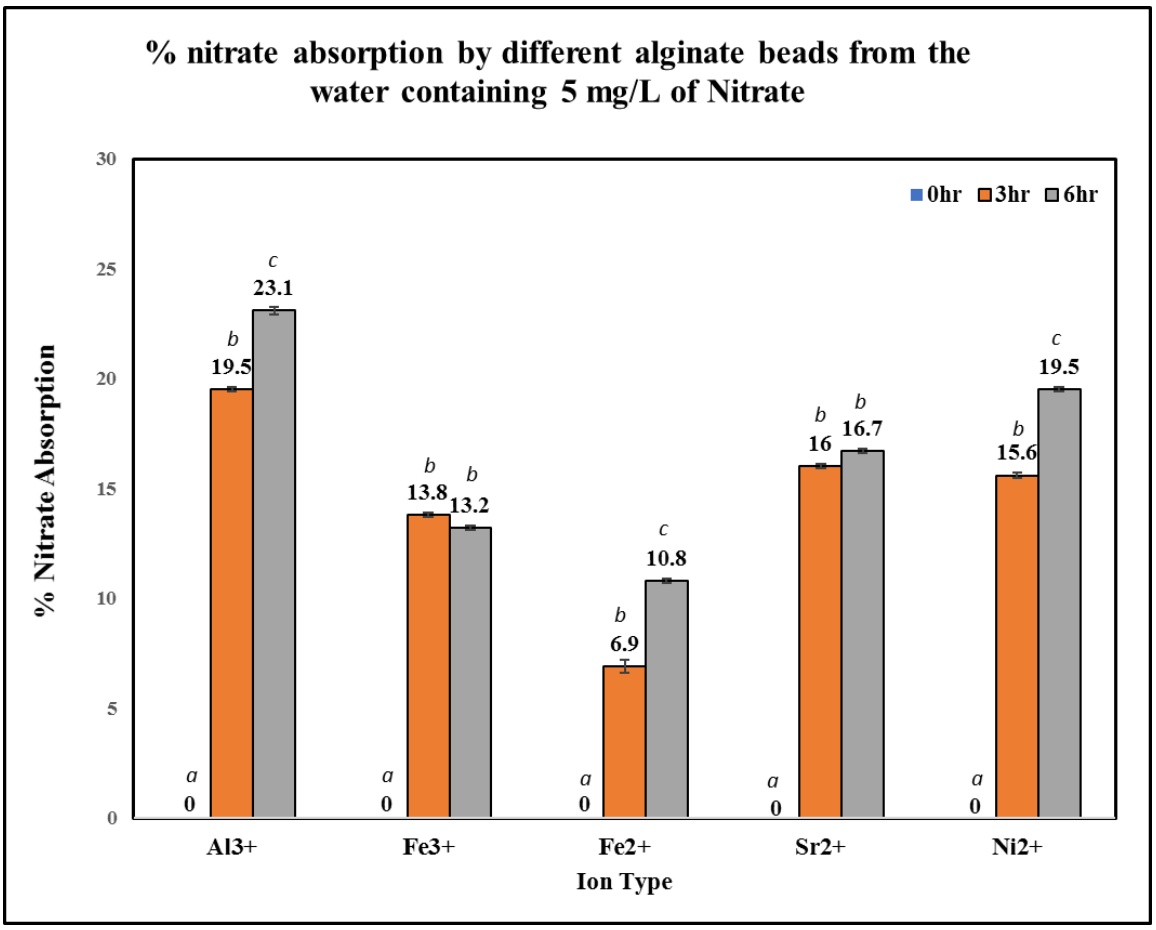

Figure 18: Percent of nitrate absorption by different alginate beads using 5 mg/L of standard nitrate water. Each bar represents mean ± SE. For each ion type, means share same letters indicate the differences are not statistically significant, while different letters indicate significantly different from each other ($p < 0.05$).

4.4. FTIR spectroscopy of the alginate beads before and after treatment with nutrients

The FTIR absorptions of sodium-alginate powder, different ionic cross-linked beads before and after nitrate and phosphate absorption have been evaluated to identify the shifts in vibrational bands, if any. The major FTIR absorptions are highlighted in Table 6 to 12. The spectra are also shown in Figure 19 to 26. The major vibrations of sodium-alginate are observed at 1018, 1404, 1604, 2931-2947, 3209-3317cm^{-1} that corresponds to -C-OH stretching, symmetric -C-O-O stretching, asymmetric -C-O-O stretching, aliphatic -C-H stretching and O-H stretching (Andrew D Clarke. 2017; S. D. Praveena 2014; Mohamed GF. 2011; JM. 2014; Pereira L. 2003). However, some additional bands are also observed at 663, 1651, 1682-1697, 1790, 2854 cm^{-1} after each type of ionic cross-linking (Table 6 to Table 12). In addition, shifting of absorption peaks before and after treatment with nitrate and phosphate are also noticed (Table 6 to Table 12).

In the case of aluminum-alginate beads the shifts of absorption peaks of 1682-1697cm^{-1} and 2916-2931cm^{-1} have been observed after capturing nitrate and phosphate which corresponds to C=O stretching and aliphatic -C-H stretching respectively.

Similar results are obtained with Fe^{2+}, Fe^{3+}, Zn^{2+}, Cu^{2+}, $Ni^{2+,}$ and Sr^{2+}ions cross-linking beads with more or less obvious shifts of absorption peaks after treatment with nitrate and phosphate. The changes in the wave numbers and observations of new peaks suggest the presence of cation in the alginate beads network.

Table 6: The major FTIR absorption (cm^{-1}) of sodium-alginate powder, aluminum-alginate beads before and after capturing nitrate and phosphate.

Na-Alginate powder	Al^{3+}-Alginate beads	Al^{3+}-Alginate beads-Nitrate	Al^{3+}-Alginate beads-Phosphate
*	663	663	663
1018	1018	1018	1018
1404	1327-1342	1342	1419
1604	1527	1527	1527
*	1651	1651	1651
*	1682-1697	1697	1697
2345-2360	2345	2345	2345
*	2854	2854	*
2931-2947	2916-2931	2916	2916
3209-3317	3595-3641	3610	3610
3672-3734	3734	3734	3734
3826-3857	3826-3857	3842	3842-3857

The absence of absorption peaks is denoted by *

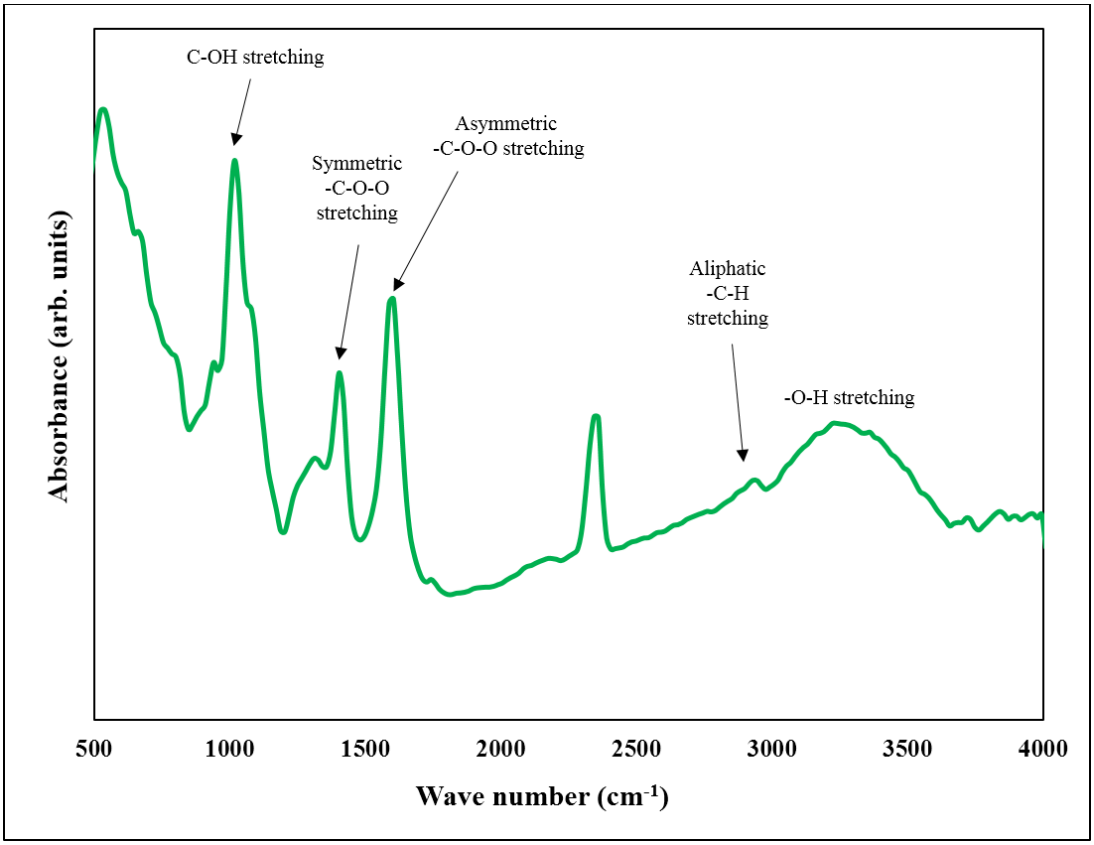

Figure 19: The FTIR spectra of sodium alginate powder

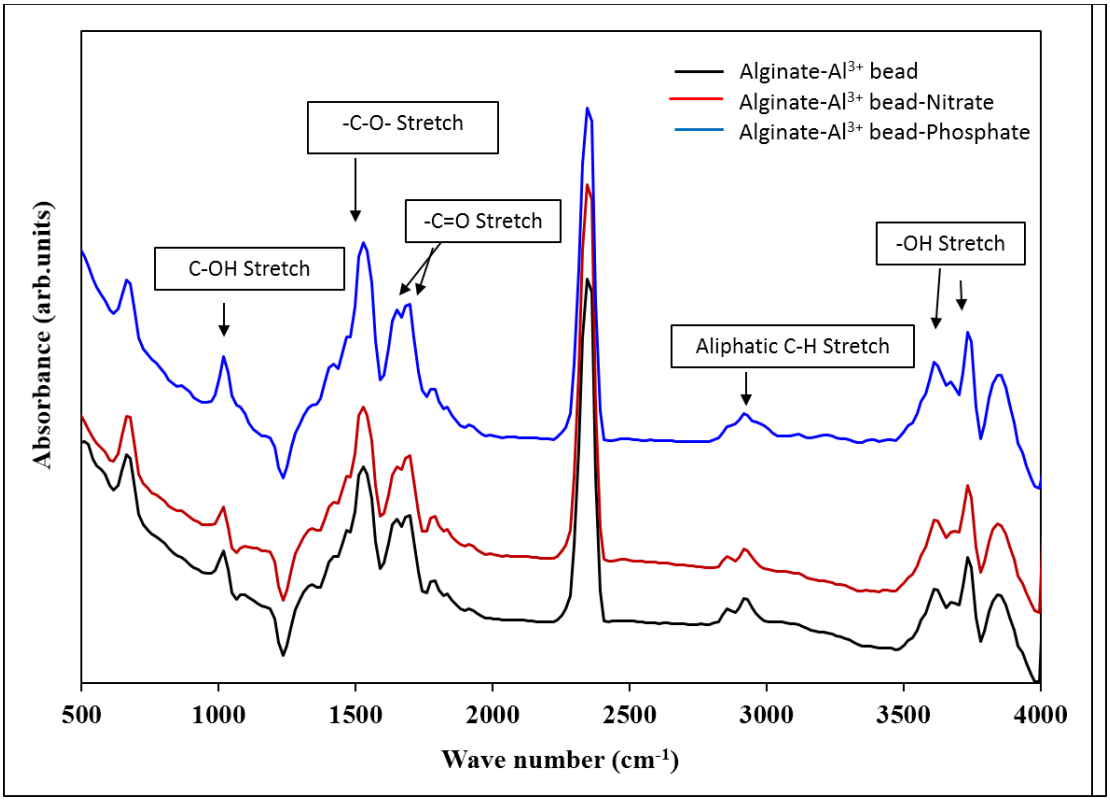

Figure 20: The FTIR spectra of aluminum-alginate beads before and after capturing nitrate and phosphate.

Table 7: The major FTIR absorption (cm^{-1}) of sodium-alginate powder, iron (II)-alginate beads before and after capturing nitrate and phosphate.

Na-Alginate powder	Fe^{2+}-Alginate beads	Fe^{2+}-Alginate beads-Nitrate	Fe^{2+}-Alginate beads-Phosphate
*	663	663	663
1018	*	1003	1018
1404	1342	1342	1419
1604	1527	1527	1527
*	1651	1651	1651
*	1697	1697	1697
*	1789	1789	1774-1789
2345-2360	2345	2345	2345
*	2854	2854	*
2931-2947	2916	2916	2916
3209-3317	3610-3626	3610-3626	3626
3672-3734	3734	3734	3734
3826-3857	3842	3842-3857	3842

The absence of absorption peaks is denoted by *

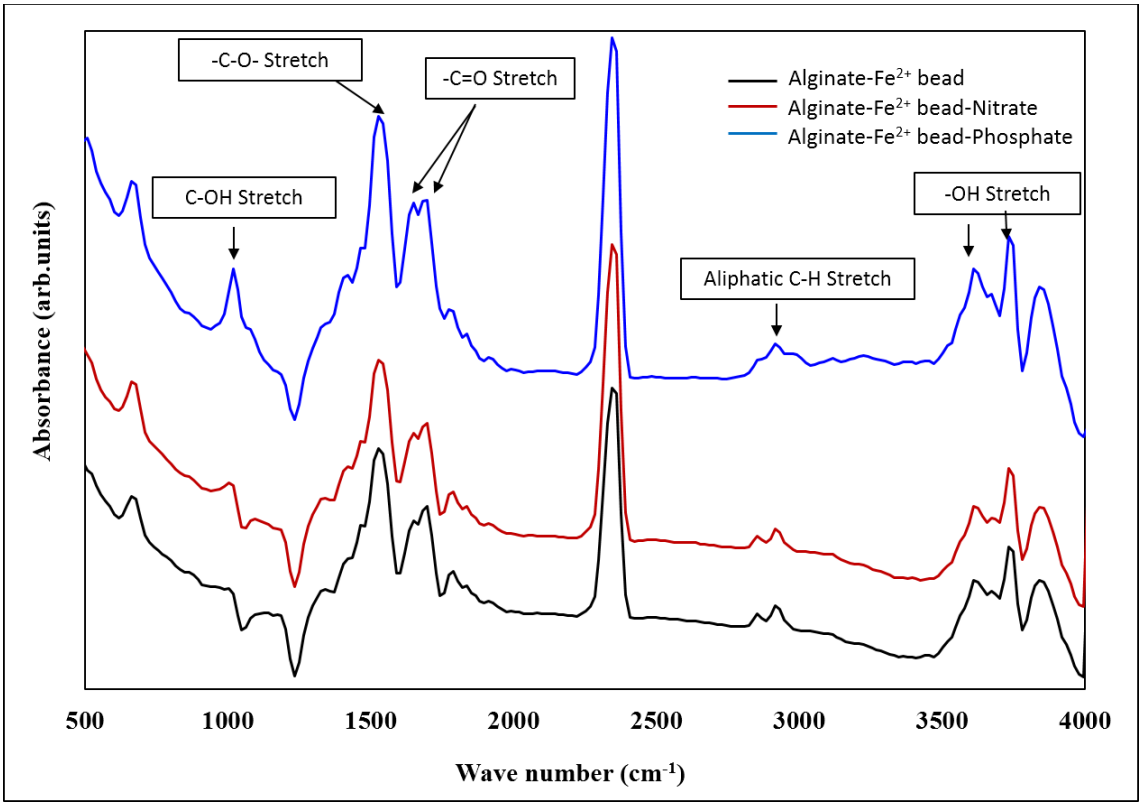

Figure 21: The FTIR spectra of iron (II)-alginate beads before and after capturing nitrate and phosphate.

Table 8: The major FTIR absorption (cm^{-1}) of sodium-alginate powder, zinc-alginate beads before and after capturing nitrate and phosphate.

Na-Alginate powder	Zn^{2+}-Alginate beads	Zn^{2+}-Alginate beads-Nitrate	Zn^{2+}-Alginate beads-Phosphate
*	663	648-679	648-679
1018	1018	1003	1018
1404	1326-1342	1326-1342	1419
1604	1527	1543	1527
*	1635-1651	1635	1651
*	1682-1697	1682	1682-1697
*	1790	1790	1774-1790
2345-2360	2345	2345	2345
*	2854	2854	*
2931-2947	2916-2931	2916	2916
3209-3317	3610	3610	3610
3672-3734	3734	3734	3734
3826-3857	3842	3842	3842

The absence of absorption peaks is denoted by *

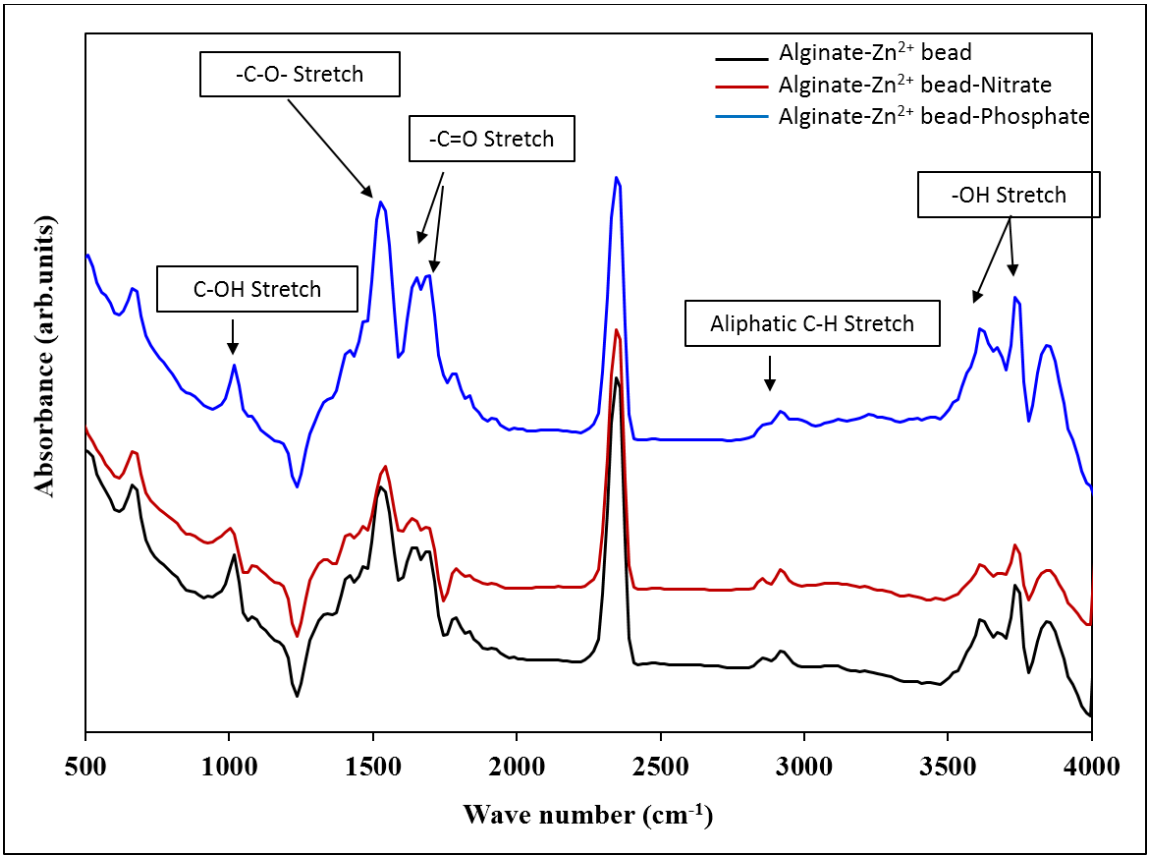

Figure 22: The FTIR spectra of zinc-alginate beads before and after capturing nitrate and phosphate.

Table 9: The major FTIR absorption (cm^{-1}) of sodium-alginate powder, iron (III)-alginate beads before and after capturing nitrate.

Na-Alginate powder	Fe^{3+}-Alginate beads	Fe^{3+}-Alginate beads-Nitrate
*	663	663
1018	1018	1018
1404	1419	1342
1604	1527	1527
*	1651	1651
*	1697	1697
*	1790	1774-1790
2345-2360	2345	2345
*	2854	2854
2931-2947	2916	2916
3209-3317	3610	3610
3672-3734	3734	3734
3826-3857	3842-3857	3842

The absence of absorption peaks is denoted by *

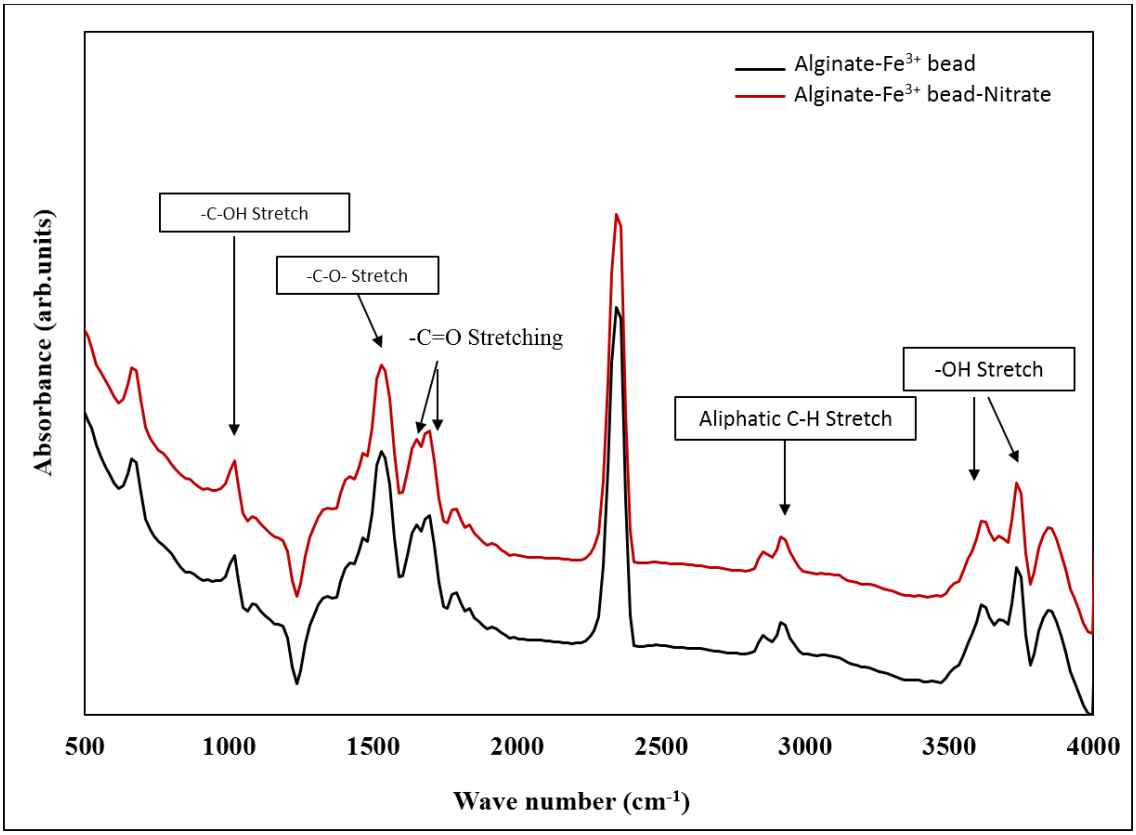

Figure 23: The FTIR spectra of iron (III)-alginate beads before and after capturing nitrate.

Table 10: The major FTIR absorption (cm^{-1}) of sodium-alginate powder, copper (II)-alginate beads before and after capturing nitrate.

Na-Alginate powder	Cu^{2+}-Alginate beads	Cu^{2+}-Alginate beads-Nitrate
*	663	663
1018	1018	1018
1404	1342	1419
1604	1527	1527
*	1651	1651
*	1697	1682-1697
*	1790	1790
2345-2360	2345	2345
*	2854	2854-2870
2931-2947	2916-2931	2916-2931
3209-3317	3610	3610
3672-3734	3734	3734
3826-3857	3842-3857	3842

The absence of absorption peaks is denoted by *

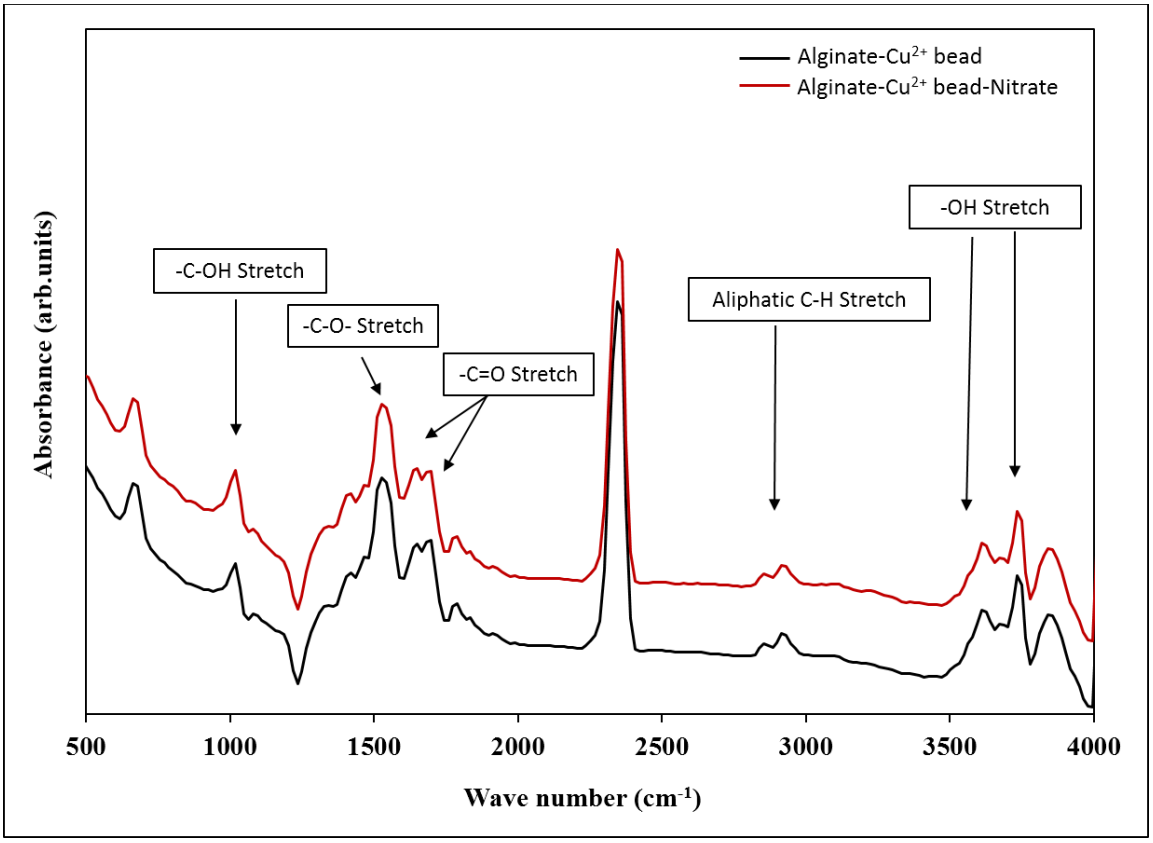

Figure 24: The FTIR spectra of copper (II)-alginate beads before and after capturing nitrate.

Table 11: The major FTIR absorption (cm^{-1}) of sodium-alginate powder, nickel-alginate beads before and after capturing nitrate.

Na-Alginate powder	Ni^{2+}-Alginate beads	Ni^{2+}-Alginate beads-Nitrate
*	663	663
1018	1018	1018
1404	1419	1404-1419
1604	1527	1574
*	1651	*
*	1682-1697	*
*	1790	1790-1805
2345-2360	2345	2345
2931-2947	2916	2916
3209-3317	3610	3610
3672-3734	3734	3734
3826-3857	3842-3857	3842

The absence of absorption peaks is denoted by *

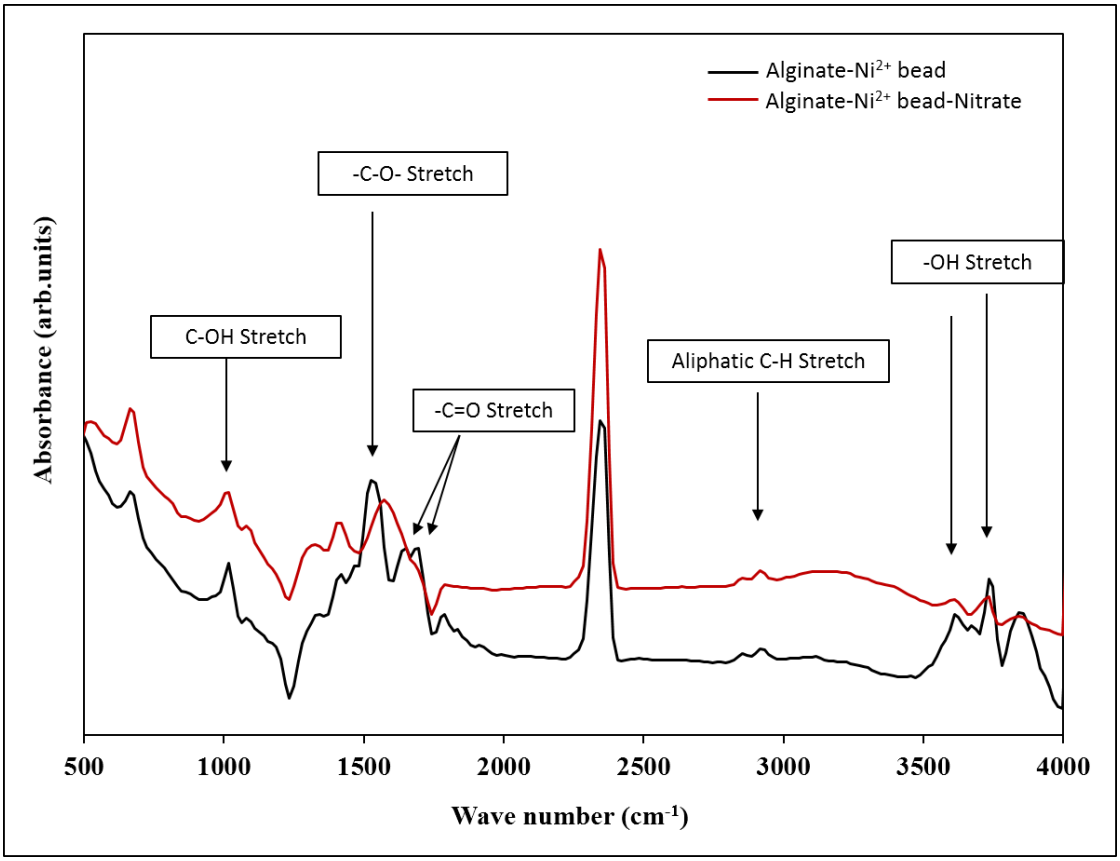

Figure 25: The FTIR spectra of nickel-alginate beads before and after capturing nitrate.

Table 12: The major FTIR absorption (cm^{-1}) of sodium-alginate powder, strontium-alginate beads before and after capturing nitrate.

Na-Alginate powder	Sr^{2+}-Alginate beads	Sr^{2+}-Alginate beads-Nitrate
*	663-679	663
1018	1018	*
1404	1342	1327-1342
1604	1527	1527-1543
*	1651	1651
*	1697	1682
*	1790	1790
2345-2360	2345	2345
*	2854	2839-2854
2931-2947	2916	2916
3209-3317	3610-3626	3610
3672-3734	3734	3734
3826-3857	3842	3842

The absence of absorption peaks is denoted by *

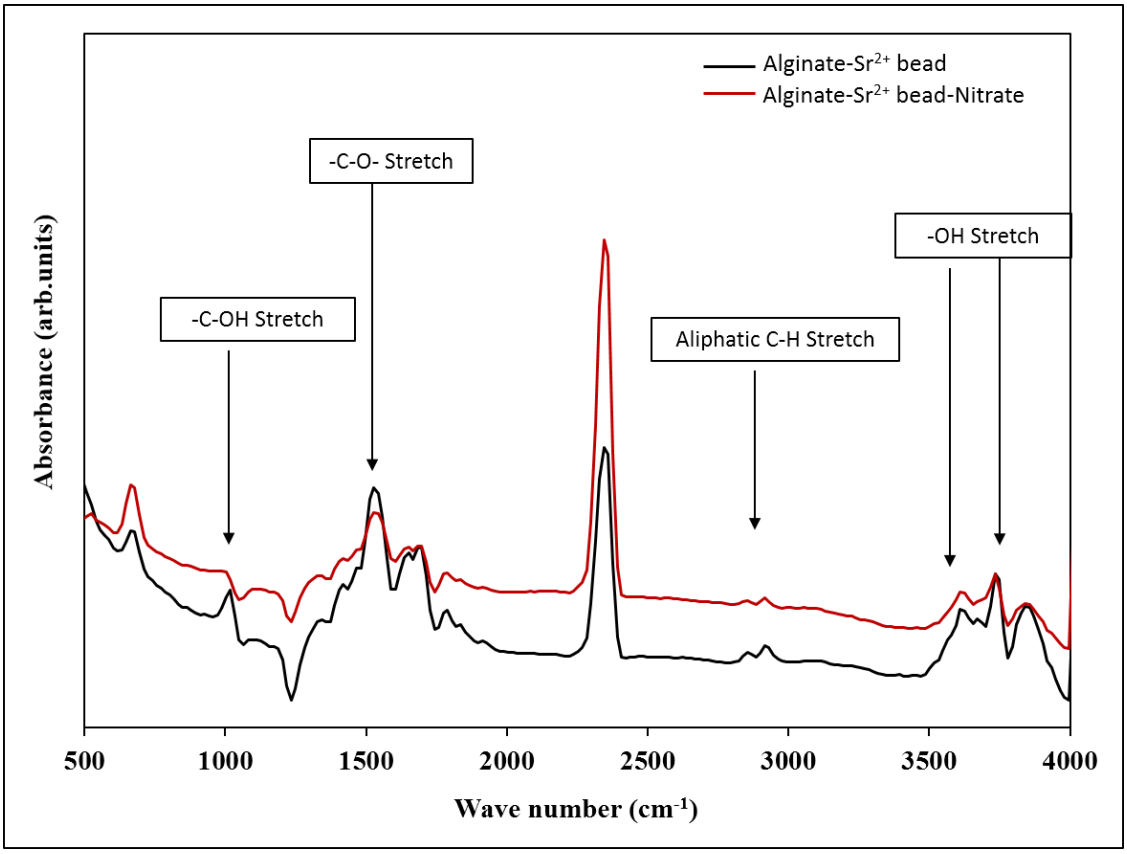

Figure 26: The FTIR spectra of strontium-alginate beads before and after capturing nitrate.

4.5. Thermal properties of alginate beads

The melting behavior of ion cross-linked alginate beads before and after treatment with nutrients are analyzed by the differential scanning calorimetry (DSC). A summary of the DSC findings is shown in Table 13 to 19. The results indicate that there is a change in the thermal properties of alginate beads after absorbing nitrate and phosphate.

The enthalpy for alginate powder is 209.9 ± 1.2 J/g and changed after cross-linking with cations. Furthermore, it has increased significantly after absorption of nitrate and phosphate (Table 13 to Table 19). The enthalpy of alginate-Al^{3+} beads is 307.4 ± 4.6 J/g before absorption of nitrate or phosphate, and it changes to 312.5 ± 6.5 J/g and 445.1 ± 0.1 J/g after absorption of nitrate and phosphate, respectively (Table 13).

Table 13: DSC of Aluminum alginate beads before and after absorption of nitrate and phosphate

Sample type	Onset Temperature(^{0}C)	Peak Temperature(^{0}C)	Enthalpy(J/g)	End Temperature(^{0}C)
Alginate	83.9 ± 0.7^a	139.2 ± 1.0^a	209.9 ± 1.2^a	198.9 ± 0.6^a
+Al^{3+}	32.3 ± 0.9^b	96.0 ± 1.5^b	307.4 ± 4.6^b	144.9 ± 0.6^b
+ Al^{3+} + NO_3^-	28.7 ± 3.1^b	105.2 ± 1.9^c	312.5 ± 6.5^b	184.6 ± 0.2^a
+ Al^{3+} + PO_4^{3-}	31.1 ± 0.1^b	104.0 ± 0.7^c	445.1 ± 0.1^c	189.7 ± 5.3^a

Each value represents mean ± SE. Means share same letters in each column indicate the differences are not statistically significant, while different letters indicate significantly different from each other ($p < 0.05$).

The enthalpy for alginate-Fe^{2+} is found to be 277.4 ± 0.3 J/g, and it significantly increases to 313.6±3.8 and 372.1±0.5 J/g after absorbing nitrate and phosphate, respectively (Table 14). Similarly, a significant change in the enthalpy of alginate-Zn^{2+} beads (153.6 ± 4.8 J/g) is also observed after capturing nitrate (202.0 ± 1.2 J/g) and phosphate (207.1 ± 5.3 J/g) (Table 15).

Table 14: DSC of Ferrous alginate beads before and after absorption of nitrate and phosphate

Sample type	Onset Temperature(^{0}C)	Peak Temperature(^{0}C)	Enthalpy(J/g)	End Temperature(^{0}C)
Alginate	83.9 ± 0.7^a	139.2 ± 1.0^a	209.9 ± 1.2^a	198.9 ± 0.6^a
+Fe^{2+}	30.1 ± 0.7^b	95.9 ± 0.1^b	277.4 ± 0.3^b	170.0 ± 1.3^b
+Fe^{2+} + NO_3^-	31.2 ± 0.6^b	106.0 ± 0.8^c	313.6 ± 3.8^c	172.0 ± 0.7^b
+Fe^{2+} + PO_4^{3-}	31.3 ± 0.7^b	106.4 ± 0.6^c	372.1 ± 0.5^d	182.1 ± 0.1^c

Each value represents mean ± SE. Means share same letters in each column indicate the differences are not statistically significant, while different letters indicate significantly different from each other ($p < 0.05$).

Table 15: DSC of Zinc alginate beads before and after absorption of nitrate and phosphate

Sample type	Onset Temperature(^{0}C)	Peak Temperature(^{0}C)	Enthalpy(j/g)	End Temperature(^{0}C)
Alginate	83.9 ± 0.7^a	139.2 ± 1.0^a	209.9 ± 1.2^a	198.9 ± 0.6^a
+Zn^{2+}	33.4 ± 0.5^b	85.5 ± 5.0^{bc}	153.6 ± 4.8^b	128.1 ± 2.7^b
+ Zn^{2+}+ NO_3^-	40.42 ± 3.9^b	106.1 ± 2.8^d	202.0 ± 1.2^a	177.4 ± 0.8^c
+Zn^{2+} + PO_4^{3-}	36.4 ± 0.4^b	98.8 ± 2.6^{bcd}	207.1 ± 5.3^a	159.0 ± 2.8^d

Each value represents mean ± SE. Means share same letters in each column indicate the differences are not statistically significant, while different letters indicate significantly different from each other ($p < 0.05$).

The enthalpy of Ferric alginate beads has significantly changed from (185.1 ± 3.6) to (296.1 ± 5.5) J/g after treating with nitrate (Table 16). Similarly, enthalpy is fluctuated for alginate beads prepared using copper, strontium, and nickel ions before and after treatment with nitrate (Table 17 to 19).

Table 16: DSC of Ferric alginate beads before and after absorption of nitrate and phosphate

Sample type	Onset Temperature(^{0}C)	Peak Temperature(^{0}C)	Enthalpy(J/g)	End Temperature(^{0}C)
Alginate	83.9 ± 0.7^a	139.2 ± 1.0^a	209.9 ± 1.2^a	198.9 ± 0.6^a
+Fe^{3+}	31.9 ± 0.6^b	92.8 ± 1.8^b	185.1 ± 3.6^b	136.0 ± 1.4^b
+Fe^{3+} + NO_3^-	25.9 ± 1.9^b	107.9 ± 2.4^c	296.1 ± 5.5^c	168.2 ± 0.2^c

Each value represents mean ± SE. Means share same letters in each column indicate the differences are not statistically significant, while different letters indicate significantly different from each other ($p < 0.05$).

Table 17: DSC of Copper alginate beads before and after absorption of nitrate

Sample type	Onset Temperature(^{0}C)	Peak Temperature(^{0}C)	Enthalpy(J/g)	End Temperature(^{0}C)
Alginate	83.9 ± 0.7^a	139.2 ± 1.0^a	209.9 ± 1.2^a	198.9 ± 0.6^a
+Cu^{2+}	32.0 ± 0.9^b	89.5 ± 2.1^b	203.3 ± 3.7^a	147.9 ± 0.9^b
+Cu^{2+} + NO_3^-	45.6 ± 3.9^c	104.4 ± 1.9^c	242.5 ± 2.5^b	164.2 ± 0.2^c

Each value represents mean ± SE. Means share same letters in each column indicate the differences are not statistically significant, while different letters indicate significantly different from each other ($p < 0.05$).

Table 18: DSC of Strontium alginate beads before and after absorption of nitrate

Sample type	Onset Temperature(^{0}C)	Peak Temperature(^{0}C)	Enthalpy(J/g)	End Temperature(^{0}C)
Alginate	83.9 ± 0.7^a	139.2 ± 1.0^a	209.9 ± 1.2^a	198.9 ± 0.6^a
$+Sr^{2+}$	31.9 ± 0.1^b	94.8 ± 2.3^b	270.0 ± 2.9^b	159.0 ± 3.1^b
$+Sr^{2+} + NO_3^-$	37.8 ± 6.3^b	108.9 ± 0.5^c	207 ± 7.1^a	172.3 ± 0.2^c

Each value represents mean ± SE. Means share same letters in each column indicate the differences are not statistically significant, while different letters indicate significantly different from each other ($p < 0.05$).

Table 19: DSC of Nickel alginate beads before and after absorption of nitrate

Sample type	Onset Temperature(^{0}C)	Peak Temperature(^{0}C)	Enthalpy(J/g)	End Temperature(^{0}C)
Alginate	83.9 ± 0.7^a	139.2 ± 1.0^a	209.9 ± 1.2^a	198.9 ± 0.6^a
$+Ni^{2+}$	31.9 ± 0.4^b	88.2 ± 1.7^b	228.2 ± 6.9^a	143.3 ± 0.8^b
$+Ni^{2+} + NO_3^-$	78.2 ± 2.6^a	142.9 ± 0.4^a	258.9 ± 3.6^b	203.5 ± 0.7^c

Each value represents mean ± SE. Means share same letters in each column indicate the differences are not statistically significant, while different letters indicate significantly different from each other ($p < 0.05$).

SUMMARY AND FUTURE RESEARCH

This study successfully establishes the proof-of-concept that alginate beads could aid in water treatment technologies. More comparative large-scale studies, however, need to be conducted to further the research concept. Indeed, findings from this research provide a strong evidence to use a specific ionic cross-linker of alginate to develop a useful tool to remove nitrate and phosphate from contaminated water. The outcome could be extended to other polysaccharides such as iota-carrageenan, kappa-carrageenan, and gellan, to name a few.

This research opens up new opportunities, mainly: (1) polysaccharide beads loaded with nutrients could be re-applied to the filed as fertilizer, adding value to farmers, and (2) Metal ions in the beads could further add value to crops as metal ions deficiency in foods is a growing health problem due to depleted soils leading to grains deprived of essential nutrients. However, further studies involving following are in need:

- Experiments need to be conducted using field water
- Research needs to be carried to enhance the nitrate absorption and holding capacity of different beads.
- These beads could be made as a large-scale filter and installed near the water streams wherein the agriculture run-off adds-in so that the nutrient contamination to the water streams could be reduced substantially.

REFERENCES

Ahiablame, L. M., I. Chaubey, D. R. Smith, and B. A. Engel. 2011. 'Effect of tile effluent on nutrient concentration and retention efficiency in agricultural drainage ditches', *Agricultural Water Management*, 98: 1271-79.

Andrew D Clarke., et al. 2017. 'Measurement of Total Sodium Alginate in Restructured Fish Products Using Fourier Transform Infrared Spectroscopy', *EC Nutrition*, 11: 33-45.

APHA. 1998. 'Standard methods for examination of water and wastewater,' *20th edn. American Public Health Association, Washington, DC*.

Arne, H.; Bjørn, L.; Olav, S. 1967. 'Studies on the Sequence of Uronic Acid Residues in Alginic Acid', *Acta Chemica Scandinavica*, 21: 691-704.

Bakhsh A., Kanwar R., Pederson, C. et al. 2007. 'N-source effects on temporal distribution of NO3-N leaching losses to subsurface drainage water', *Water, Air, and Soil Pollution*, 181: 35-50.

Berkessa, Yifru Waktole, Seid Tiku Mereta, and Fekadu Fufa Feyisa. 2019. 'Simultaneous removal of nitrate and phosphate from wastewater using solid waste from factory', *Applied Water Science*, 9.

Blann, Kristen L., James L. Anderson, Gary R. Sands, and Bruce Vondracek. 2009. 'Effects of Agricultural Drainage on Aquatic Ecosystems: A Review', *Critical Reviews in Environmental Science and Technology*, 39: 909-1001.

Clark, D. E.; Green, H. C. 1936. "Alginic acid and process of making same." In. US Patent.

Dinnes, D.L., Karlen, D.L., Jaynes, D.B., Kaspar, T.C., Hatfield, J.L., Colvin, T.S., Cambardella, C.A.,. 2002. 'Nitrogen management strategies to reduce nitrate leaching in tile-drained Midwestern soils', *Agron. J.*, 94: 153–71.

Drury, C. F., C. S. Tan, J. D. Gaynor, T. O. Oloya, and T. W. Welacky. 1996. 'Influence of Controlled Drainage-Subirrigation on Surface and Tile Drainage Nitrate Loss', *Journal of Environment Quality*, 25.

El-Naas, M. H., Al-Zuhair, S., Al-Lobaney, A., Makhlouf, S. 2009. 'Assessment of electrocoagulation for the treatment of petroleum refinery wastewater', *Journal of Environmental Management.*, 91: pp.180-85.

Fewtrell, L. 2004. 'Drinking-water nitrate, methemoglobinemia, and global burden of disease: a discussion', *Environ Health Perspect*, 112: 1371-4.

Foglar, L., Briski, F., Sipos, L., Vukovic, M. 2005. 'High nitrate removal from synthetic wastewater with the mixed bacterial culture', *Bioresource Technology*, 96: pp. 879-88.

Galvez, J. M., Gomez, M. A., Hontoria, E., Gonzalez-Lopez, J. 2003. 'Influence of hydraulic loading and air flowrate on urban wastewater nitrogen removal with asubmerged fixed-film reactor asubmerged fixed-film reactor', *Journal of Hazardous Materials.*, 101: pp. 219-29.

Georg Jensen, M., M. Kristensen, A. Belza, J. C. Knudsen, and A. Astrup. 2012. 'Acute effect of alginate-based preload on satiety feelings, energy intake, and gastric emptying rate in healthy subjects', *Obesity (Silver Spring)*, 20: 1851-8.

Gomez, M. A., Galvez, J. M., Hontoria, E., Gonzalez-Lopez, J. 2003. 'Influence of concentration on biofilm bacterial composition from a denitrifying submerged filter

used for contaminated groundwater', *Journal of Bioscience Bioengineering.*, 95: pp. 245-51.

Goolsby, et. al. 1999. 'Flux and Sources of Nutrients in the Mississippi–Atchafalaya River Basin: Topic 3 Report for the Integrated Assessment on Hypoxia in the Gulf of Mexico.', *NOAA Coastal Ocean Program Decision Analysis Series No. 17.*: 130.

Grant, G. T., Morris, E. R., Rees, D. A., Peter, Smith, J. C., Thom, D. . 1973. 'Biological interactions between polysaccharides and divalent cations: The egg-box model', *FEBS Letters*, 32: 195-98.

Greer, F. R., M. Shannon, Nutrition American Academy of Pediatrics Committee on, and Health American Academy of Pediatrics Committee on Environmental. 2005. 'Infant methemoglobinemia: the role of dietary nitrate in food and water', *Pediatrics*, 116: 784-6.

Gunay, A., Karadag, D., Tosun, I. & Ozturk, M. 2008. 'Use of magnesit as a magnesium source for ammonium removal from leachate', *Journal of Hazardous Materials*, 156: 619–23.

Guo, C. H., V. Stabnikov, and V. Ivanov. 2010. 'The removal of nitrogen and phosphorus from reject water of municipal wastewater treatment plant using ferric and nitrate bioreductions', *Bioresour Technol*, 101: 3992-9.

Heathwaite, A. L., and R. M. Dils. 2000. 'Characterising phosphorus loss in surface and subsurface hydrological pathways', *Sci Total Environ*, 251-252: 523-38.

Helness, H., and H. Odegaard. 2001. 'Biological phosphorus and nitrogen removal in a sequencing batch moving bed biofilm reactor', *Water Sci Technol*, 43: 233-40.

Henderson, C., M. Greenway, and I. Phillips. 2007. 'Removal of dissolved nitrogen, phosphorus and carbon from stormwater by biofiltration mesocosms', *Water Sci Technol*, 55: 183-91.

Hua, G., M. W. Salo, C. G. Schmit, and C. H. Hay. 2016. 'Nitrate and phosphate removal from agricultural subsurface drainage using laboratory woodchip bioreactors and recycled steel byproduct filters', *Water Res*, 102: 180-89.

Hyun-Joon Kong, Kuen YongLee, David JMooney. 2002. 'Decoupling the dependence of rheological/mechanical properties of hydrogels from solids concentration', *Polymer*, 43: 6239-46.

JM., Pereira L and Neto. 2014. 'Analysis by vibrational spectroscopy of seaweed with potential use in food, pharmaceutical and cosmetic industries.' in Pereira L and PJ. Ribeiro-Claro. Boca Raton (ed.), *Marine algae: biodiversity, taxonomy, environmental assessment, and biotechnology"* (Taylor and Francis Group, LLC).

Keeney, D. R., Hatfield, J. L., . 2008. 'Chapter 1. The Nitrogen Cycle, Historical Perspective, and Current and Potential Future Concerns', *USDA-ARS / UNL Faculty*: 262.

Kim, D., Ryu, H. D., Kim, M. S., Kim, J., Lee, S. I. . 2007. 'Enhancing struvite precipitation potential for ammonia nitrogen removal in municipal landfill leachate', *Journal of Hazardous Materials*, 146: pp. 81–85.

KIM, Hae-Sung. 1990. 'KINETIC STUDY ON CALCIUM ALGINATE BEAD FORMATION', *Korean J of Chem. Eng.*, 7: 1-6.

Kim, T., Park, S., Shin, E., Kim, S. 2002a. 'Decolorization of disperse and reactive dyes by continuous electrocoagulation process', *Desalination*, 150: pp. 165-75.

Kim, Y. S., Nakano, K., Lee, T. J., Kanchanatawee, S., Matsumura, M. . 2002b. 'On-site nitrate removal of groundwater by an immobilized psychrophilic denitrifier using soluble starch as a carbon source', *Journal Bioscience Bioengineering*, 93: pp. 303-08.

King, K. W., M. R. Williams, and N. R. Fausey. 2015. 'Contributions of systematic tile drainage to watershed-scale phosphorus transport', *J Environ Qual*, 44: 486-94.

Kioussis, D. R., Kofinas, P. . 2005. 'Characterization of anion diffusion in polymer hydrogels used for wastewater remediation', *Polymer*, 46: pp. 9342-47.

Kioussis, D. R., Wheaton, F. W., and Kofinas, P. 2000. 'Reactive nitrogen and phosphorus removal from aquaculture wastewater effluents using polymer hydrogels', *Aquacultural Engineering*, 23: pp. 315-32.

Kohler, J. 2001. 'Detergent phosphates and detergent ecotaxes: a policy assessment', *Centre Européen d'Etudes des Polyphosphates-a European Chemical Industry Council (CEFIC) sector group.*: pp 6-9.

Kuo, C. K., and P. X. Ma. 2008. 'Maintaining dimensions and mechanical properties of ionically crosslinked alginate hydrogel scaffolds in vitro', *J Biomed Mater Res A*, 84: 899-907.

Lee, K. Y., and D. J. Mooney. 2012. 'Alginate: properties and biomedical applications', *Prog Polym Sci*, 37: 106-26.

Li, R., J. Niu, X. Zhan, and B. Liu. 2013. 'Simultaneous removal of nitrogen and phosphorus from wastewater by means of FeS-based autotrophic denitrification', *Water Sci Technol*, 67: 2761-7.

Malakootian, M. and Yousefi, N. 2009. 'The efficiency of electrocoagulation process using aluminum electrodes in removal of hardness from water', *Iran Journal of Environmental Health and Science Engineering.*, 6: pp. 131–36.

Maurer, M., Boller, M. . 1999. 'Modelling of phosphorus precipitation in wastewater treatment plants with enhanced biological phosphorus removal', *Water Science Techology.*, 39: pp. 147-63.

Mohamed GF., et al. 2011. 'Application of FT-IR Spectroscopy for Rapid and Simultaneous Quality Determination of Some Fruit Products ', *Nature and Science*, 9: 21-31.

Moore, Julie. 2016. 'Literature Review: Tile Drainage and Phosphorus Losses from Agricultural Land', *Lake Chamberlain Basin Program*, TECHNICAL REPORT NO. 83.

Mousavi, S. A. R., Ibrahim, S., Arouna, M. K., Ghafari, S. 2011. 'Bio-electrochemical denitrification- A review', *International Journal of Chemical and Environmental Engineering*, 2: pp. 140-45.

Park, H. I., Kim, D. K., Choi, Y. J., Pak, D. . 2005. 'Nitrate reduction using an electrode as direct electron donor in a biofilm electrode reactor', *Process Biochemistry*, 40: pp.3383-88.

Patel, N., D. Lalwani, S. Gollmer, E. Injeti, Y. Sari, and J. Nesamony. 2016. 'Development and evaluation of a calcium alginate based oral ceftriaxone sodium formulation', *Prog Biomater*, 5: 117-33.

Pereira L., et al. 2003. 'Use of FTIR, FT-Raman and 13 C-NMR spectroscopy for identification of some seaweed phycocolloids', *Bioorganic Chemistry*, 20: 223-28.

Prosnansky, M., Sakakibara, Y. and Kuroda, M. 2002. 'High-rate denitrification and SS rejection by biofilm-electrode reactor (BER) combined with microfiltration', *Water Research*, 36: pp. 4801-10.

Rabalais, et al. 2002. 'Gulf of Mexico Hypoxia, A.K.A. "The Dead Zone"', *Annual Review of Ecology and Systematics*, 33: 235-63.

Ranjan, S. et al. 2016. 'Selective Removal of Nitrate and Phosphate from Wastewater Using Nanoscale Materials', *Sustainable Agriculture Reviews*, 23.

Rosellini, E., C. Cristallini, N. Barbani, G. Vozzi, and P. Giusti. 2009. 'Preparation and characterization of alginate/gelatin blend films for cardiac tissue engineering', *J Biomed Mater Res A*, 91: 447-53.

S. D. Praveena, V. Ravindrachary, R. F. Bhajantri, I. Ismayil. 2014. 'Free volume-related microstructural properties of lithium perchlorate/sodium alginate polymer composites', *Polymer Composites*, 35: 1267-74.

Sarparastzadeh, H., Saeedi, M., Naeimpoor, F., Aminzadeh, B. 2007. 'Pretreatment of Municipal Wastewater by Enhanced Chemical Coagulation', *International Journal of Environmental Reserach.*, 1: pp.104-13.

Shrimali, M., Singh, K.P. 2001. 'New methods of nitrate removal from water', *Environmental Pollution*, 112: pp. 351-59.

Sims, J. T., Vasilas, B. L., Gartley, K. L., Milliken, B., and Green, V. 1995. 'Evaluation of Soil and Plant Nitrogen Tests for Maize on Manured Soils of the Atlantic Coastal Plain', *Agronomy Journal*, 87: 213-22.

Soares, J. P. C.; Santos, J. E. V.; Chierice, G. O.; Cavalheiro, E. T. G. 2004. 'Thermal behavior of alginic acid and its sodium salt', 29: 53-56.

Szekeres, S. 2001. 'Hydrogen-dependent denitrification in a two-reactor bioelectrochemical system', *Water Research*, 35: pp. 715-19.

Takeshita, S.; Oda, T. . 2016. 'Marine Enzymes Biotechnology: Production and Industrial Applications, Part II - Marine Organisms Producing Enzymes', *Advances in Food and Nutrition Research*, 79: 137-60.

Tchobanoglous, G., Burton, F. L., Stensel, H. D. 2003. 'Wastewater Engineering: Treatment, Disposal, and Reuse.', *Meltcalf & Eddy, Inc. 4th edition. New York: McGrawHill, Inc.*: pp.1819.

Torsdottir, I., M. Alpsten, G. Holm, A. S. Sandberg, and J. Tolli. 1991. 'A small dose of soluble alginate-fiber affects postprandial glycemia and gastric emptying in humans with diabetes', *J Nutr*, 121: 795-9.

Van Rijn, J., Tal, Y., and Schreier, H.J., . 2006. 'Denitrification in recirculating systems: Theory and applications', *Aquacultural Engineering*, 34: pp. 364-76.

Vijayalakshmi, S.; Sivakamasundari, S.K.; Moses, J.A.; Anandharamakrishnan, C. . 2019. *Potential Application of Alginates in the Beverage Industry* (WILEY).

WHO. 1985. 'Health Hazards from nitrates in drinking water.', *World Health Organization, Copenhagen,*: 73–94.

Xiong, Y., Strunk, P., Hongyun, X., Xihai, Z., Karlsson, H. 2001. 'Treatment of dye wastewater containing acid orange II using a cell with three-phase three-dimensional electrode', *Water Research*, 35: pp. 4226-30.

Yamashita, T., and R. Yamamoto-Ikemoto. 2014. 'Nitrogen and phosphorus removal from wastewater treatment plant effluent via bacterial sulfate reduction in an anoxic

bioreactor packed with wood and iron', *Int J Environ Res Public Health*, 11: 9835-53.

Zhang, L., Jia, J., Zhu, Y., Zhu, N., Wang, Y., and Yang, J. . 2005. 'Electro-chemically improved bio-degradation of municipal sewage', *Biochemical Engineering Journal*, 22: pp. 239-44.

Zhao, L., G. You, F. Liao, X. Kan, B. Wang, Q. Sun, H. Xu, D. Han, and H. Zhou. 2010. 'Sodium alginate as viscosity modifier may induce aggregation of red blood cells', *Artif Cells Blood Substit Immobil Biotechnol*, 38: 267-76.